THE EFFECT OF SURFACE MODIFICATION OF BIOMATERIALS ON THE CELLULAR INTERACTIONS

A Thesis Submitted to
the Graduate School of Engineering and Sciences of
İzmir Institute of Technology
in Partial Fulfillment of the Requirements for the Degree of

MASTER OF SCIENCE

In Biotechnology

by
Melek ÖZGÜR

February 2008
İZMİR

We approve the thesis of **Melek ÖZGÜR**

Prof.Dr.Muhsin ÇİFTÇİOĞLU
Supervisor

Prof.Dr.Şebnem HARSA
Co-Supervisor

Prof.Dr.Serdar ÖZÇELİK
Committee Member

Assoc.Prof.Dr.Oğuz BAYRAKTAR
Committee Member

01.02.2008

Date

Prof.Dr. Semra ÜLKÜ
Head of the Biotechnology Department

Prof.Dr. Hasan BÖKE
Dean of the Graduate School of
Engineering and Sciences

ACKNOWLEDGEMENTS

I would like to thank and express my deepest gratitude to Prof.Dr. Muhsin Çiftçioğlu for his supervision, guidance and encouregement thruoghout my thesis work. I also wish to thank Prof.Dr.Şebnem Harsa for her valuable suggestions and comments about this thesis.

I am very grateful to specialist Rukiye Çiftçioğlu for her endless help, support and tolerance in the laboratory work. This work would never be complete without her contribution, understanding and skills.

Finally I am grateful to my engaged and family members, for their encouragement, endless support and understanding throughout my study.

ABSTRACT

THE EFFECT OF SURFACE MODIFICATION OF BIOMATERIALS ON THE CELLULAR INTERACTIONS

The preparation and characterization of chitosan-hydroxyapatite composite scaffolds and protein adsorption chracteristics of these scaffolds have been investigated in this study. The effects of different chitosan/hydroxyapatite contents of the low density composites on the protein adsorption behaviour were experimentally examined. Bradford method at 595 nm and 280 nm UV protein absorption methods were used for the determination of adsorbed amount of bovine serum albumin (BSA) and human serum protein (HSP). In this study low molecular weight chitosan and hydroxyapatite have been used for the preparation of the scaffold composites by freeze drying and SEM was used for microstructural analysis. The thermal behaviour of the composites was investigated by DSC and TGA. Composite scaffolds were prepared by using different amounts of chitosan and hydroxyapatite (HA) and six different scaffolds were prepared and coded as C100H0, C80H20, C70H30, C50H50, C30H70, and C20H80. The porous low density scaffolds had 93.5-96.3% porosity with a slight increase in density with increasing HA content. The interconnected pore network was formed from 50-250 μm relatively uniform size pores with thin pore walls. The HA particles were fully embedded in the polymer matrix in the pore walls. The TGA curves have shown that the freeze dried phase seperation induced biopolymer sturucture degrates at lower temperatures faster than the original raw polymer.

The adsorptions of BSA and HSP onto composites have been studied as a function of time, protein concentration and pH. Adsorption experiments were also conducted with commercial HA powder. The adsorption kinetics experiments have indicated that protein adsorption was almost completely achieved in the first 2-3 hours with relatively high uptake values of up to 45-60 mg/g and 40-60 mg/g for 595 nm Bradford and 280 nm methods. The adsorption behaviour did not fit to the commonly known Langmuir and Freundlich isotherms. This was attributed to the swelling/degradation tendency of the freeze-dried chitosan containing scaffolds. The HSP uptake of 30 and 50 wt% HA containing composites were in the 50-60 mg/g range which was higher than other composites and the raw unprocessed chitosan.

ÖZET

BİYOMALZEMELERİN YÜZEY MODİFİKASYONUNUN HÜCRESEL ETKİLEŞİMLERE ETKİSİ

Bu çalışmada kitosan-hidroksiapatit (HA) yapı iskelesi kompozitlerinin hazırlanması-karakterizasyonu ve protein adsorplama özellikleri araştırılmıştır. Bu düşük yoğunluklu malzemelerde değişen kitosan ve HA içeriğinin protein adsorplama davranışına etkileri incelenmiştir. Adsorplanan BSA ve HSP protein konsantrasyonları 595 nm Bradford ve 280 nm absorbsiyona dayalı UV metotlarıyla saptanmıştır. Düşük molekül ağırlıklı kitosan ve HA bu gözenekli malzemelerin dondurmalı kurutmayla eldesinde kullanılmış ve malzemelerin mikroyapıları SEM kullanılarak incelenmiştir. Kompozitlerin ısıl davranışları TGA ve DSC kullanılarak saptanmıştır.

Kompozit yapı iskeleleri değişen ağırlık oranlarında kitosan ve HA kullanılarak hazırlanmış ve altı değişik malzeme C100H0, C80H20, C70H30, C50H50, C30H70 ve C20H80 olarak kodlanmıştır. Gözenekli çok düşük yoğunluklu yapıların 93.5-96.3 % gözeneğe sahip oldukları ve artan HA içeriğiyle yoğunluklugun ufak bir artış gösterdiği saptanmıştır. Kompozitlerin birbirine bağlantılı gözenek yapısının düzenli 50-250 μm boyutunda gözenekler ve ince gözenek duvarları içerdiği ve HA parçaçıklarının duvarlarda tamamen gömülü olduğu SEM incelemelerinde görülmüştür. Faz ayırma metodu ile üretilen biyopolimer yapısının orijinal ham polimerden düşük sıcaklıklarda daha hızlı parçalandığı TGA eğrilerinden gözlenmiştir.

Kompozitlere BSA ve HSP adsorpsiyonu zaman, protein konsantrasyonu ve pH'nın değişimine karşılık incelenmiştir. Adsorpsiyon deneyleri aynı zamanda ticari HA tozuylada yürütülmüştür. Adsorpsiyon kinetiğiyle ilgili deneyler protein adsorsiyonunun hemen hemen 2-3 saat içerinde tamalandığını ve 595 nm Bradford ve 280 nm protein UV absorpsiyonu metotlarına gore protein alımının 45-60 mg/g ve 40-60 mg/g gibi yüksek düzeylere ulaşabildiğini göstermiştir. Kompozitlerin adsorpsiyon davranışlarının yaygın olarak bilinen Langmuir ve Freundlich izotermlerine uymadığı saptanmıştır. Bunun nedeninin dondurarak kurutulan kitosanın sulu ortamda şişmesi/bozunması olduğu düşünülmüştür. Yapı iskelelerinden 30 ve 50% HA içeren kompozitlerin HSP adsorpsiyon alımları 50-60 mg/g aralığında diğer örneklerden ve işlenmemiş kitosandan yüksek olarak saptanmıştır.

TABLE OF CONTENTS

LIST OF FIGURES

LIST OF TABLES

CHAPTER 1

INTRODUCTION

There is a necessity for replacing bone substance which has been lost due to traumatic or nontraumatic events (Suchanek, et al. 1998). The implanted biomaterial must have certain desired properties in order to achieve a satisfactory result and to have an appropriate host response at the hard tissue implantation site. The microstructural and mechanical properties of the bone must be thoroughly understood for the successful preparation of canditate hard tissue implant biomaterials in order to mimic the natural bone structure.

Reconstructive treatment of the bone defects is a widespread practice. Several kinds of materials can be used in these procedures: autografts (obtained from the patient itself) allografts (homografts from humans, xenografts from animals), or implants made out of bone bonding biomaterials. Autologous vascularized bone grafts are the 'golden standard', but morbidity and pain at donor sites, the limited number of donor sites, the limits in size of the bone graft joined to the costs and time of a double surgery, have shifted the interest towards allografts. Allografts are not immune from drawbacks besides bacterial contamination. The major disadvantages of allografts includes the risk of induction of transmissible diseases in the recipient, and the graft tendency to elicit immune response which can lead to high failure rates. As a consequence the interests has shifted towards the use of implantable biomaterials, characterized by bone bonding properties and by a morphology simulating the one of cancellous bone.

A biomaterial is any substance or combination of substances, which can be used for any period of time, as a whole or as a part of a system for use in the human body to measure, restore, and improve physiologic function, and enhance survival and quality of life. Typically, inorganic (metals, ceramics, and composites) and polymeric (synthetic and natural) materials have been used for such items as artificial heart-valves, (polymeric or carbon-based), synthetic blood-vessels, artificial hips (metallic or ceramic), medical adhesives, sutures, dental composites, and polymers for controlled slow drug delivery. Biomaterials must be compatible with body in order to exhibit their function properly. The use of incompatible materials as medical implants in the body

may induce unfavourable immune reactions, undesirable interactions with blood and other body fluids as well as damaging the genetic material at the chromosomal and DNA levels.

Material biocompatibility is an essential prequisite for a successful functioning of any implant. Since the application area of biomaterials has been increasing rapidly, the interest for these materials has been also increasing which caused the development and the use of several biocompatibility testing methods to evaluate the biocompatibility of materials. The initial necessary phase of biocompatibility involves the adsorption of blood serum proteins onto the biomaterial surfaces. Protein adsorption is generally regarded as a primary event that occurs when the material comes into contact with biological surroundings (Suchanek, et al. 1998).

Hard tissue of the human body is very important. The skeletal system provides support and gives shape to the body and provides a network for soft tissue attachment. The most common problems that are faced in hard tissues are bone fractures in addition to various other problems. The developments in artificial bone preparation techniques may solve most of the hard tissue problems. On the other hand artificial bones themselves may cause other problems and in many cases they do not have sufficient mechanical properties.

Ceramics, polymers, metals and composite materials are developed to be used as bone implants along with their advantages and disadvantages. Polymers have very low mechanical strength compared to bone, metals have superior mechanical properties but they are very corrosive, and despite their other desired properties such as wear resistance, biocompatibility and hardness, ceramics are brittle and have low fracture toughness. When all these properties of polymers, ceramics and metals are considered producing composite materials is a reasonable approach.

Bone consists of 69 wt % calcium phosphate (mainly hydroxyapatite (HA)), 21% collagen, 9%water and 1% other constituents. It has a composite nature which is composed of mainly ceramic and polymeric components with a complex hierarchical microstructure difficult to imitate which gives most of the superior mechanical properties to bone. Extensive research has been conducted on bone substitute composite materials composed of mainly hydroxyapatite and a polymer. Hydroxyapatite has excellent bioactivity, biocompatibility, non-toxicity and osteoconductivity properties but also has low toughness. Chitosan, deacetylated form of chitin, is a natural polymer found in vast amounts in crustaceans. It is biocompatible and

bioresorbable/biodegradable. It is non-toxic and easily soluble in dilute weak organic acids. The recent research on chitosan/hydroxyapatite composites which are partially biodegradable indicate that this behaviour of the composite may even be an advantage. New bone may intergrow around the hydroxyapatite particles when the polymer matrix is resorbed. Extensive research on relatively new chitosan/hydroxyapatite composites has been conducted recently (Zhao, et al. 2007).

The objective of this study was the preparation and characterization of polymeric/ceramic porous composite biomaterials by using chitosan and hydroxyapatite along with also the investigation of the protein adsorption behaviour of these composites. The effects of parameters such as HA and chitosan contents on BSA (Bovine Serum Albumin) and also HSP (Human Serum Protein) adsorption behaviour have been ivestigated which was considered to be a prerequiste for biocompatibility.

CHAPTER 2

BIOMATERIALS AND BIOCOMPATIBILITY

2.1. Biomaterials

A biomaterial is defined as a non-viable material used in the production of medical devices and intending to interact with biological systems. Biomaterials, natural or synthetic in origin, can be used for any period of time or permenantly. Their function is to treat or replace any tissue, organ or function of the body. It is known that many materials have been used as potential biomaterials for surgical glues, stents, external fixation devices, wound dressing, and dental materials. These implants can be metallic, polymeric, composite or ceramic in nature. The selection of materials used for implants is very important with respect to their function in the body (Bosetti, et al. 2001).

Ceramics are mainly used for the repair, reconstruction and replacement of diseased or damaged parts of the body especially in the mucolo-skeletal system such as bone. Main characteristics of ceramics for their use as biomaterials are their relatively high compressive strengths, biocompatibility, inertness, pore and crystalline structure but they are brittle and difficult to produce. Hydroxyapatite is a highly biocompatible ceramic which can be processed in dense or porous structure similar to natural bone. HA is widely used as a bone filling material and to coat the surfaces of metallic prosthetic implants in order to improve their biocompatibility. It has been demonstrated that the physical characteristics of HA particles (size, shape) could modify the toxicity of biomaterials in the above applications (Grandjean-Laquerriere, et al. 2004). Al_2O_3 (α-alumina) is also a bioceramic widely used clinically. It is used in total hip prosthesis and dental implants because of its combination of excellent corrosion resistance, good biocompatibility, low friction, high wear resistance, and high strength (Hench 1998).

Metals are also desired due to their mechanical properties for load bearing parts of body. Typical examples of highly loaded implants are hip and knee endoprothesis. In addition, metalic materials are also used for unloaded and functional devices such as heart valves (Hu, et al. 2004). Metals are known to be tough and ductile. The main disadvantages of these materials are poor corrossion resistance and their relatively high density. The release of metal ions to the body may induce biological reactions including

oxidative damage to lipids, proteins, and DNA because of the increase in the concentration of reactive oxygen species and depletion of intracellular anti-oxidants. They can also cause apoptosis (cell death), inflammation (initial reaction of the body involving redness, swelling), and mutation. With the combination of other materials or coating with inert materials, biocompatibility, corrosion and wear resistance can be improved and they can be used for a long time in the body safely (Hu, et al. 2004). The most frequently used metals nowadays are stainless steel (316L stainless steel) and titanium because of their high biocompatibility and corrosion resistance. Zinalco composed of 80% zinc, 18% aluminium, and 2% copper is very similar to 316L stainless steel and titanium due to its physical and mechanical properties. In vitro and in vivo test results have shown that zinalco is harmless and can be used as potential biomaterial (Aguilar, et al. 1999). Mechanical properties of some important biomaterials are given in Table 2.1. The types, advantages and disadvantages of biomaterials are given in Table 2.2.

Table 2.1. Mechanical properties of some metallic and ceramic materials
(Source: Ramakrishna, et al. 2001)

Material	Modulus (GPa)	Tensile Strength (MPa)
Stainless Steel	190	586
Co-Cr Alloy	210	1085
Ti Alloy	116	965
Amalgam	30	58
Alumina	380	300
Zirconia	220	820
Bioglass	35	42
Hydroxyapatite	95	50

Table 2.2. Types and properties of biomaterials

Materials	Advantages	Disadvantages	Examples
Polymers Nylon Silicones	Resilient Easy to fabricate Bioresorbable, bioinert	Insufficient properties for load bearing applications, Deform with time May degrade	Sutures, blood vessels, hip socket, ear, nose
Metals Titanium Co-Cr alloys Stainless steel	High strength, tough, ductile	corrosive, dense	Joint replacement, bone plates and screws, dental root implants
Ceramics Alumina Carbon Hydroxyapatite	Biocompatible, inert, strong in compression, wear resistant, bioactive	Brittle, difficult to produce, not resilient, high modulus	Dental, hip socket
Composites	High strength, controllable mechanical properties and microstructure	Difficult to produce	Joint implants, heart valves

Tissue engineering studies widely use polymeric materials with the aim of production of artificial organs and prothesis because of their high elasticity and simplicity in production. Poly (3-hydroxybutyric acid-co-3-hydroxyvaleric acid) (PHBV) is a natural polyester polymerized by the bacteria. This polyester is biodegradable and biocompatible. PHBV can be used for biomedical applications including surgical sutures, wound dressings, vascular grafts, and scaffols for new tissue in growth (Hu, et al. 2004). Chitosan is the deacetylated derivative of chitin and one of the most abundant natural polysaccharides. It has been identified as hydrophilic, non-toxic, biodegradable, and antibacterial. It has been used as wound dressing accelerator and immune system stimulant. Cyanoacrylates are also polymers used in the production of medical devices that have several advantages: they are easy and rapid to be applied, relatively painless and they eliminate the need for suture removal. Poly (vinyl-pyrolidone) has interesting properties as well: immediate pain control, easy replacement, transparancy to allow healing follow up, and barrier against bacteria. Polyurethane and silicone are also most common polymers for implants such as stents and catheters.

There are many efforts to improve physical and mechanical properties of biocompatible materials. Composites are materials composed of two or more distinct materials in order to obtain stronger, tougher, more durable and biocompatible materials. Risbud, et al. (2001) have studied the biocompatibility of poly (butylene terephthalate)/wollastonite composite which is a biodegradable engineering plastic exhibiting bone-bonding properties, titanium implant coating, and dental implant applications. Wollastonite is a naturally occurring calcium silicate and it is known to be bioactive. Wollastonite has been reported to enhance the mechanical performance of composites. The difficulties in production of composites are the main drawback of these materials.

Polymer–ceramic composite scaffolds such as chitosan-hydroxyapatite composites are excpected to mimic natural bone. The hydroxyapatite–chitosan–alginate porous network has been also reported and demonstrated to be suitable for bone tissue engineering applications using osteoblast cells (Manjubala, et al. 2006).

2.2. Biocompatibility

The materials used in devices must be safe in addition to being effective. This characteristic or property of a material is termed as biocompatibility. Biocompatibility may generally be regarded as the ability of a material to interact with living cells/tissues or a living system by not being toxic, injurious, or causing immunological reactions while performing or functioning appropriately. The spectrum of biomaterials used in medical applications is quite broad. They range from cotton pads that stop bleeding of minor cuts within a few minutes; to catheters, dialysis tubes, contact lenses designed to interact with tissues from a few hours to weeks. They range from sutures designed to slowly resorb over a few weeks to months; to implant devices like total replacement hips and heart valves intended to last 10–15^{+} years or the lifetime of the patient. To encompass this diversity of materials and applications, a consensus panel of experts has defined biocompatibility as “the ability of a material to perform with an appropriate host response in a specific application” (Pariente, et al. 1998). This definition thus accounts for not only the variety of applications of materials in medical devices, but also for the responses of both host tissues to material and material to host tissues.

The determination of the biocompatibility of materials and implant devices involves detailed characterization of the material (e.g., bulk and surface chemical composition; density; porosity; and mechanical, electrical, and degradation properties) and extensive testing, first at the protein/cell/tissue or in-vitro level, and then in in-vivo animal models and ultimately in human clinical trials. In-vitro tests are used to screen materials, their components, and or leachable/soluble/degradation products for cytotoxic, genotoxic, immunological, and hemolytic effects. Animal models are used to evaluate material–host tissue interactions and to predict how the device or prototype may perform in humans. Ultimately, the safety and effectiveness of the device must be evaluated in humans prior to widespread use by physicians and their patients. At each stage, biocompatibility testing results must be correlated with materials properties and with manufacturing, sterilization, packaging, storage, and other handling procedures that also may influence test outcomes.

The design and use of biocompatibility testing protocols are provided by a variety of professional and regulatory organizations including ASTM (American Society for Testing and Materials International), ISO (International Standards Organization), ADA (American Dental Association), NIH (National Institutes of Health), and FDA (Food and Drug Administration). The use and documentation of biocompatibility tests are required by law in the United States and other countries, and are used to ensure that biomedical devices and their constituent materials are safe and effective under intended application conditions.

2.3. Bone

2.3.1 Structure and Composition of the Bone

Bone is a specialized connective tissue with mineralized extracellular matrix (ECM). Bone grafting is routinely performed to restore bone loss due to trauma or disease. Although autogenous cancellous bone is considered to be the gold standard for bone grafts, there are several limitations, including inadequate availability, increased operative blood loss from the two-site surgery, and potential donor-site morbidity. Allogeneic grafts are also problematic due to risks in infection, allograft fracture, pathogen transmission, and immune rejection. It has, therefore, become necessary to

find suitable alternatives, particularly when a large graft is required. Bone tissue engineering is a promising alternative to bone grafting. In the tissue engineering approach, the following components are generally required: cells that can differentiate into osteoblasts, an artificial extracellular matrix (ECM; i.e., scaffold), and regulating bioactive molecules that promote cell recruitment, growth, differentiation, and mineralized bone tissue formation (Zhang, et al. 2001). These components have to be in concert with each other to achieve optimal tissue regeneration.

The extracellular matrices (ECMs) of hard tissues are composed of organic and inorganic phases, the inorganic phase consisting primarily of HA crystals, and the organic phase consisting mainly of type I collagen and small amounts of other substance including glycosaminoglycans (GAGs), proteoglycans and glycoproteins.

Table 2.3. The composition of the bone
(Source: Park, et al. 1992)

Component	**Amount (wt %)**
Hydroxyapatite	69%
Organic matrix • Collagen • Others	22% 90-96% of organic matrix 4-10% of organic matrix
Water	9%

Bone is difficult to analyze because it has so many levels of organization. The main constituents of bone are collagen (21 wt. %), calcium phosphate (69 wt. %) as given in Table 2.3. Additionally, water and other organic materials such as proteins, polysaccharides and lipids are also present in small quantities. Collagen which can be considered as the matrix is in the form of small microfibers. It is difficult to observe distinct collagen fibers because of its net-like mass appearence. The diameter of collagen microfiber varies from 100 to 2000nm (Suchanek, et al. 1998). The hydroxyapatite crystals are present in the form of plates or needles which are about 40-60 nm long, 20 nm wide and 1.5-5 nm thick. They are arranged parallel to the collagen fibers, such that the larger dimension of crystals axis along the axis of fiber.There is a hierarchical structure which can be seen in Figure 2.1. (Park, et al. 1992).

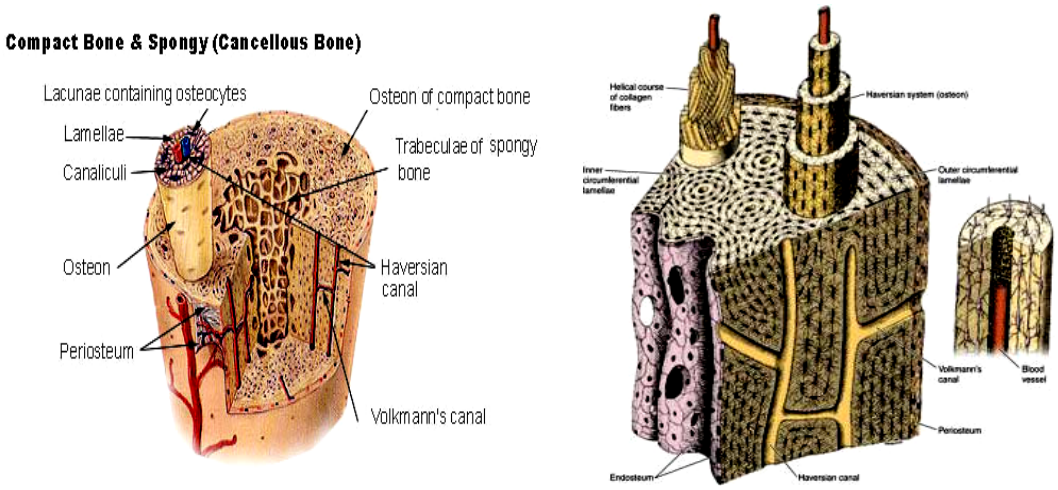

Figure 2.1. Organisation of Bone (a) Compact and Cancellous (b) Compact (Source: Park, et al. 1992)

Bone consists of two main parts, compact bone, also known as cortical bone, and the cancellous bone, also known as trabecular or spongy bone. Compact bone is the outer surface of the human bone. It is harder and denser compared to the spongy bone. Cancellous bone is softer and has lower density compared to the compact bone. The mineral-containing fibers are arranged into lamellar sheets (3-7 μm thick) 4-20 lamelae, which are arranged in concentric rings around the Harversian Canal, form an osteon (Suchanek, et al. 1998).

The metabolic substances can be transported by the intercommunicating systems of canaliculi, lacunae, and Volkman's canals, which are connected with the narrow cavity. The various interconnecting systems are filled with body fluids and their volume can be as high as 19% (Suchanek, et al. 1998).

Due to the properties mentioned, there is not a homogeneous composition and all the properties/compositions are directionally and regionally dependent.

2.3.2. Mechanical Properties of Bone

Bones of the skeletal system provide the supporting structure for the body. The low elastic modulus collagen fibers are aligned in bone along the main stress direction. The high elastic modulus hydroxyapatite mineral includes approximately 70 % of the

dry bone mass and contributes significantly to the bone stiffness. Bone can remodel and adapt itself to the applied mechanical environment, which is generally known as Wolff's Law which is the principle relating the internal structure and architecture of the bone to external mechanical stimuli. Remodeling of bone takes place in response to mechanical stimulation so that the new structure becomes suitably adapted to the load. Density of living bone is influenced by the stress condition applied to the bone. Higher applied stress leads to the denser bone, conversely if the applied stress is lower than the normal physiological load, the bone mass decreases and leads to bone weakening. Bone is an anisotropic material as longitudinal mechanical properties of cortical bone are higher than the transverse direction properties. Bone is generally weak in tension and shear, particularly along the longitudonal plane (Ramakrishna, et al. 2001).

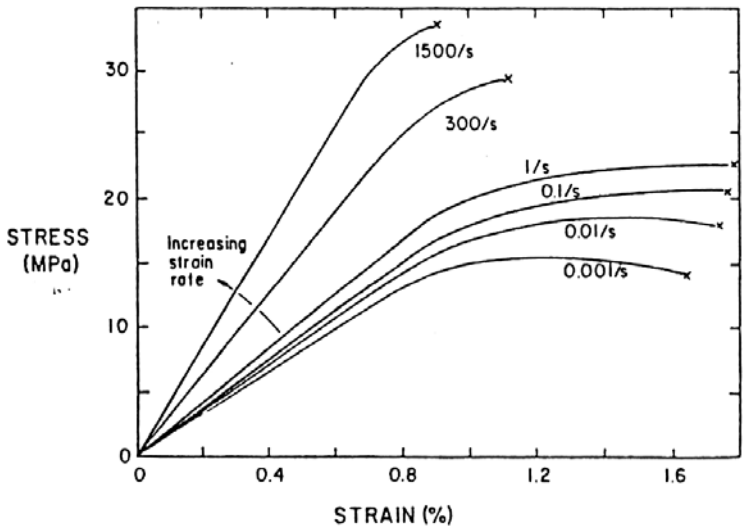

Figure 2.2. Stress as a function of strain and strain rate for human compact bone (Source: Park, et al. 1992)

Bone exhibits excellent toughness (at low strain rates) mostly due to its hierarchical structure, which stops cracks after a little propagation. The main toughening mechanism seems to be microcracks, which appear in the plastic region of the stress-strain curve. The stress strain curves of bone due to changing strain rates are given in Figure 2.2. (Park, et al. 1992).

The mechanical properties of bone depend largely on the humidity, mode of applied load, direction of the applied load, and the kind of bone. With increasing level

of bone mineralization, strength increases. Moreover, strength and other mechanical properties of bone depend on orientation of the collagen fibers, bone density, and porosity, molecular structure and arrangement of its constituent apatite crystals within their collagen matrix (Suchanek, et al. 1998). Both strength and volume of human bone decrease dramatically with age.

CHAPTER 3

CHITOSAN / HYDROXYAPATITE COMPOSITES

3.1. Chitosan

Chitosan as a natural biopolymer, is a potential candidate for tissue engineering and drug delivery systems. It is one of the most abundant naturally occurring polysaccharides, primarily obtained as a sub-product of seafood, containing amino and hydroxyl groups. The primary unit of chitin is 2-acetamido–2-deoxy-D-glucose, while that of chitosan is 2-amino-2-deoxy-D-glucose with β→1-4 glucosidic linkages. In Figure 3.1. the sructures of chitin and chitosan are shown. Generally, chitin is obtained from crustaceans or mollusks and as mentioned before chitosan is prepared from its *N*-deacetylation.

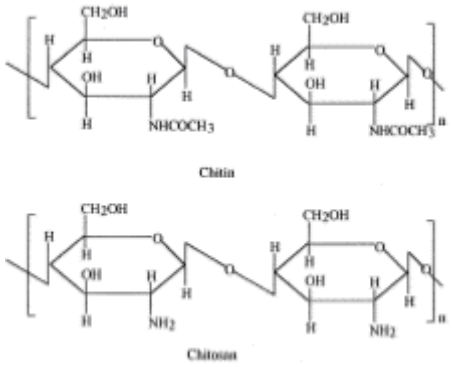

Figure 3.1. Structure of chitin and chitosan

Chitosan is insoluble in water, alkali and many organic solvents but soluble in many dilute aqueous solutions of organic acids, of which most commonly used are formic acid and acetic acid. Apart from being bioresorbable it is biocompatible, non-toxic, non-antigenic and biofunctional (Zhang, et al. 2001). Chitosan has been proposed to serve as a non-protein matrix for 3D tissue growth. Chitosan could provide the biological primer for cell-tissue proliferation and reconstruction. One of the most promising features of chitosan is its excellent ability to be processed into porous structures for use in cell transplantation and tissue regeneration. In tissue engineering,

the porous structure of chitosan provides a scaffold for bone cells to grow in and seed new bone regeneration. For rapid cell growth, the scaffold must have optimal micro architecture such as pore size, shape and specific surface area. Therefore the major goal in fabricating scaffolds for bone tissue engineering is to accurately control pore size and porosity. Porous chitosan structures can be formed by freezing and lyophilising chitosan–acetic acid solutions in suitable moulds. Pore orientation can be directed by controlling the geometry of thermal gradients during freezing. The use of chitosan scaffolds in tissue engineering has been reported and a porous chitosan matrix has been suggested as a potential candidate for bone regeneration due to its biological and physical properties.

Under acidic conditions, chitosan in its original form adopts a positive charge which can attract negatively charged plasma proteins leading to platelet adhesion and activation followed by thrombus formation and blood coagulation This sequential response should partly be responsible for the success of chitosan in wound healing acceleration. Antimicrobial activity is believed to originate from the ability of cationic species to bind with sialic acid in phospholipids, consequently restraining the movement of microbiological substances. Oligomeric chitosan can also penetrate into the cells of micro-organisms and prevent the growth of cells by prohibiting the transformation DNA into RNA (Manjubala, et al. 2006).

3.2. Hydroxyapatite

Pure HA [$Ca_{10}(PO_4)_6(OH)_2$] has the theoretical composition of: 39.68 wt % Ca, 18.45 wt % P, Ca/P weight ratio of 2.151 and Ca/P molar ratio of 1.67 (Hench, et al. 1993).

The term apatite describes a family of compounds having similar structures but not necessarily having identical compositions. Apatite is a description not a composition. Hydroxyapatite also named as calcium hydroxyapatite has a definite composition and a crystallographic structure. Hydroxyapatite belongs to the hexagonal system, with a space group, $P6_3/m$. This space group is characterized by a six-fold c-axis perpendicular to three equivalent a-axes (a_1, a_2, a_3) at angles 120^o to each other. Unit cell consists of Ca, PO_4, and OH groups closely packed together (Hench, et al. 1993). Figure 3.2. represents the crystal structure of hydroxyapatite.

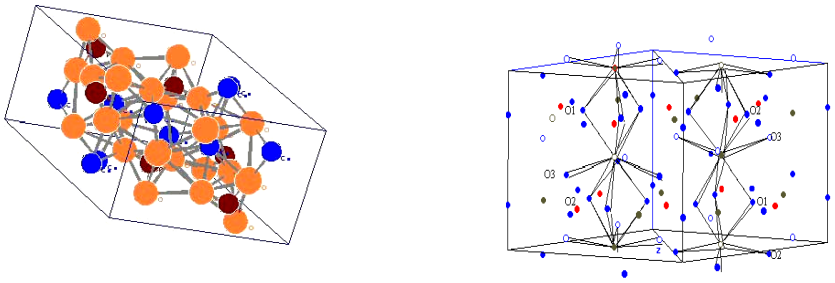

Figure 3.2. Schematic of crystal structure of hydroxyapatite (hexagonal)

From the point of view of biocompatibility, hydroxyapatite seems to be the most suitable ceramic material for the hard tissue replacement implants since hydroxyapatite is the main mineral constituent of teeth and bones. Hydroxyapatite ceramics do not have any toxic effects. They show excellent biocompatibility with hard tissues and also with skin and muscle tissues and HA can directly bond to bone. Unfortunately due to the low reliability, especially in wet environments the HA ceramics cannot presently be used for heavy load bearing applications, like artificial teeth or bones. There has been extensive research towards increasing the mechanical reliability of HA.

3.3. Chitosan / Hydroxyapatite Composites

As a consequence of tumors, infections, trauma, or other causes, bone defects need to be repaired. An ideal clinical bone substitute material should be nontoxic, biocompatible with all the tissues, including bone and blood, around it, and osteoconductive to form a good environment in the interface of mature bone and the implant, and maintain good mechanical properties in the wet state (Zhao, et al. 2007).

The research on chitosan/HA composite biomaterials for hard tissue applications has been conducted for the last 5 years whereas other bioresorbable composite materials have been in clinical use for about 15 years which is also a relatively short time. This is a promising area beause use of bioresorbable polymer ceramic composites have many advantages. The main drawback of such materials is insufficient mechanical properties compared to bone.

Hydroxyapatite (HA) based materials, having a similar chemical composition to that of the mineral phase of bone, are excellent candidates for bone repair and regeneration and have been used in bone tissue engineering for the last two decades. Though HA (Ca10(PO4)6(OH)2) is bioactive and osteoconductive, its mechanical properties are inadequate, making it unable to be used as a load bearing implant (Park, et al. 1992). In order to achieve controlled bioactivity and biodegradability, polymer–ceramic composites have been proposed. Polymers such as chitosan have a higher degradation rate than bioceramics. Incorporation of HA into a chitosan polymer matrix has also been shown to increase osteoconductivity and biodegradability with significant enhancement of mechanical strength (Park, et al. 1992). To combine the osteoconductivity of calcium phosphate and good biodegradability of polymers, composites have been developed for bone tissue engineering (Suchanek, et al. 1998). Polymer–ceramic composite scaffolds are expected to mimic natural bone, in the way that natural bone is also a composite of inorganic compounds (calcium phosphates especially substituted carbonated hydroxyapatite) and organic compounds (collagen, protein matrix, etc.), (Manjubala, et al. 2006).

3.3.1. Processing of Chitosan / Hydroxyapatite Composites

The preparation and characterization of chitosan/HA composites to be used as hard tissue implants have been investigated in the literature. There are several preparation techniques for chitosan/HA composites. Commonly used methods are phase separation (freeze drying), precipitation, sol-gel and using bone cement formulations.

Zhao, et al. (2007) investigated the preparation of three dimensional hydroxyapatite/chitosan-gelatin network composite scaffolds produced by phase separation method. A suspension was prepared by using pulverized hydroxyapatite and deionized distilled water. After 0.5 h stirring at room temperature the suspension was treated ultrasonically until the HA powder was thoroughly dispersed in the water. Chitosan and acetic acid were added under agitation. After stirring overnight gelatin was added to this suspension which was held in 40^{o}C water bath. After addition of a glutaraldehyde solution the mixture was put into plastic petri dishes at 4^{o}C half an hour then rapidly transferred to a freezer at –40^{o}C to solidify the solvent and induce solid-liquid phase separation. Solidified mixture was maintained at that temperature for 2 hours and placed in a freeze-drier. The sample was finally freeze-dried for at least 30h

and the prepared foam were cut into discs. Changing the HA content and the compositional variables of the original suspension allowed control of the porosities and densities of the scaffold as tabulated in Table 3.1.

Table 3.1. The porosities and densities of the prepared CS-Gel/HA scaffolds (Source: Zhao, et al. 2007)

CS-Gel concentration (w/v)%	CS-Gel/HA Ratio (w/w)%	Quenching Temperature (^oC)	Density (kg/m^3)	Porosity (%)
1.0	50/50	-20	0.042±0.017	95.8±8.3
2.5	50/50	-20	0.083±0.09	93.4±11.5
5.0	50/50	-20	0.156±0.011	90.6±6.8
7.5	50/50	-20	0.237±0.05	85.2±3.9
2.5	70/30	-20	0.078±0.010	94.7±8.7
2.5	30/70	-20	0.091±0.013	91.0±7.2
2.5	50/50	-80	0.092±0.011	91.8±5.9

In another study by Ang et al., three dimensional chitosan-hydroxyapatite scaffolds were prepared by using a robotic dispensing system. The dispensing material was prepared by dissolving chitosan in acetic acid and adding HA to obtain different HA/chitosan ratios to form a hydrogel. The mixture was stirred for 2h and transferred to a vacuum oven (preset at 37^{o}C) to remove air bubbles. By using the robotic dispensing machine the dispensing materials were extruded into a dispensing medium. The extruded 3D scaffolds were immersed in ethanol for 5 min and washed 3 times with distilled water. The scaffolds were then rapidly transferred to a freezer at –20 ^{o}C to solidify solvent so as to induce a solid liquid phase separation. The frozen scaffolds were maintained at –20 ^{o}C for at least 8h and then freeze dried at –56 ^{o}C for 2 days to remove the solvent. In vitro cell culture study was performed for biocompatibility characterization.

Zhang, et al. (2001) prepared chitosan scaffolds reinforced by calcium phosphates by phase separation method. Chitosan solutions with concentration of 2 wt% were prepared by dissolution of chitosan in acetic acid solution. The mixture was stirred

at 50 ^{o}C for 2h to obtain a homogeneous polymer solution. Calcium phosphate invert glass and β-TCP powders were added into the solution. The final composition of the composite foam was determined by the concentration of the chitosan solution and calcium phosphate content in the mixture. The mixture was then rapidly transferred into a freezer (–20 ^{o}C) to solidify the solvent and induce solid liquid phase separation. The solidified mixture was maintained at that temperature for 8h and the frozen mixture was then transferred into a freeze-drier at –5 ^{o}C preset temperature. The samples were freeze dried at 0.5 mmHg for at least 4 days to completely remove the solvent. In their study the effect of the chitosan content on mechanical properties, physical properties and in vitro observation was investigated.

CHAPTER 4

ADSORPTION

4.1. Adsorption, Adsorptive, Adsorbent

Adsorption is the adhesion of molecules on the surfaces of solids. Adsorption was defined as the enrichment of one or more components in an interfacial layer. Solid material on which solutes of interest adhere is called as the adsorbent. The material in the fluid phase which is capable of being adsorbed is called the adsorptive. The material adsorbed on the solid is called as the adsorbate.

When the mixture to be separated is brought into contact with another insoluble phase, the adsorbent, an unequal distribution of the original constituents between the adsorbed phase on the solid surface and the bulk of the fluid occur which permits separation. The adsorption often occurs as a monolayer on the surface of the adsorbent. However, several layers sometimes occurs.

There are two types of adsorption phenomena: physical and chemical adsorption. Characteristic features of physical and chemical adsorption are shown in Table 4.1.

Physical adsorption is a reversible phenomena which is a result of inter molecular forces of attraction between molecules of solid and adsorbate. These forces involved in physical adsorption include both Van der Waals forces (dispersion-repulsion) and electrostatic interactions comprising polarisation, dipole and quadropole interactons. In the case of some adsorbents with an ionic structure, besides Van der Waals forces, electrostatic interactions are also significant.

Chemisorption is the result of the chemical interactions between the adsorbent and the adsorbate. The strength of the chemical bond may vary considerably. The force of adhession is usually much grater than that found in physical adsorption.

Table 4.1. Characteristic features of physical and chemical adsorption

Physical adsorption	**Chemical adsorption**
Low heat of adsorption (<2 or 3 times latent heat of evaporation)	High heat of adsorption (>2 or 3 times latent heat of evaporation)
Non specific	Highly specific
Monolayer or multilayer	Only monolayer
No dissociation of adsorbed species. Only significant at relatively low temperatures	May involve dissociation possible over a wide range of temperatures
Rapid	Slow
Non activated	Activated
Reversible	İrreversible
No electron transfer although polarization of adsorbate may occur.	Electron transfer leading to bond formation between adsorbate and surface

Desorption is opposite of adsorption and the amount adsorbed decreases if the difussion is in the opposite direction, mass transfer from adsorbent to the fluid phase, desorption takes place. When the reverse isotherm does not follow the same path of adsorption, adsorption hysteresis evolves.

Adsorbents must posses certain engineering properties depending upon the application. Many adsorbents have been devoleped for a wide range of separations. Typically, adsorbents are in the form of small pellets, beats, or granules ranging from about 0.1 mm to 12 mm in sizes. The performence of an adsorption process depends heavily on the capacity of the adsorbent.

Adsorbents must have large surface area. The amount they adsorb is roughly proportional to the surface area of the adsorbent which nessecitates the condition that they must have porous structures. Pore sizes and total pore volume of adsorbents are very important as well as shape of the pores.

The following classification of pores according to width have been commonly adopted in the literature:

- Macropores (>50 nm)
- Mesopores (2-50nm)
- Micropores (<2nm)

In addition to these properties, the usefullness of an adsorbent is a function of the composition, hydrophilicity-hydrophobicity, the nature of present ligands or other functional groups, the mechanical and chemical stability of the adsorbent. The adsorbents used in bioprocesses should also be biocompatible, resistant to microorganisms, sterilizable, and stable.

Different adsorbents utilize different bonding mechanisms. Adsorbents can be classified in three main groups as inorganic (silica, carbon, calsium phosphate, zeolites, etc.), synthetic polymers or resins (dextran, poysulfone, etc.), and composites (silica-dextran, hydroxyapatite-chitosan, etc.).

Inorganic adsorbents such as activated carbon, silica and alumina are generally rigid, stable and available in many sizes and shapes. The selectivity however is rather low, regeneration is also difficult and the life time is limited. Activated carbon has non polar surfaces that are used to adsorb nonpolar molecules especially hydrocarbons. Activated alumina which has a polar surface is largely used as a dessicant. HA is used for proein purification.

The most important class of inorganic adsorbents is probably zeolites, a subclass of moleculer sieves. They are crystalline aluminasilicates with specific pore sizes located within small crystals.

Synthetic polymers are prepared by polymerizing monomers. They are avaiable in a gel and macroreticular sponge like structure. They are used in a wide range of applications such as in the recovery of antibiotics and adsorbing organic and inorganic

pigments etc. Their mechanical strength, especially that of gel type limits their applicability in large scale processes and they are mainly used in chromotography.

The composite adsorbents combine the disadvantages of the inorganic rigid carrier with the favourable adsoption behavior of polymeric adsorbents. The inner surface of an inorganic carrier is covered with a very thin layer of an organic material. Composite adsorbents can be applied in the recovery of proteins.

4.2. Adsorption Equilibra

The analysis of adsorption is based on equilibria and on mass balance. The equilibria are presented as adsorption isotherms at constant temperature. The amount adsorbed varies with concentration. This relation betwen the amount adsorbed on the solid and concentration in the fluid is called as an isotherm.

Typical isotherms for various materials for liquid adsorption are shown in Figure 4.1.

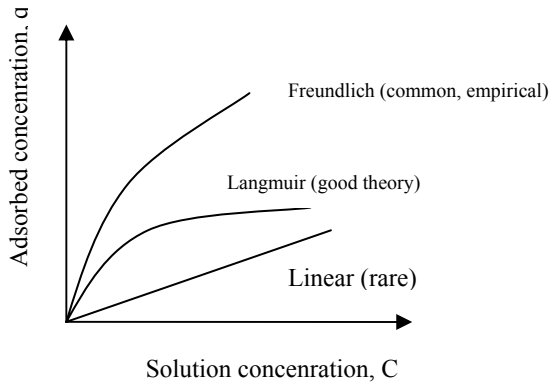

Figure 4.1. Common adsorption isotherms

For each isotherm, the abcissa gives the solute concentration in the solution in units of mass of solute per volume of solution. The ordinate gives the solute concentration on the surface of the adsorbent most commonly in units of mass of solute per mass of adsorbent. Any isotherm with a downward curvature is referred to as favorable and any isotherm with an upward curvature is referred to as unfavourable.

The determination of adsorbtion isotherm is important in providing data such as maximum capacity of adsorbent and dissociation constant. The linear isotherm can be expressed by an equation similiar to Henry's law:

$$q = K.c \tag{1}$$

where q is the amount of solute adsorbed per amount of adsorbent, c is the solute concentration in solution, K is a constant determined experimentally in volume of solution per mass of adsorbent. This linear isotherm is not common but in dilute region it can be used to approximate data of many systems.

The Freundlich isotherm equation, which is empirical often approximates data for many physical adsorption systems and is particularly useful for liquids.

$$q = K.c^n \tag{2}$$

where K and n are constants and must be determined experimentally if a log-log plot of q versus c is made, the slope is the dimensionless exponent n. The dimensions of K depend on the value of n.

The Langmuir isotherm has a theoretical basis and it is given by:

$$q = \frac{q_m.c}{K + c} \tag{3}$$

Where q_m and K are again constants. The dimensions of q_m and K are the same as those of q and c respectively. K and q_m must be determined experimentally. By plotting l/q versus l/c the slope gives K/ q_m and the intercept is l/ q_m.

q_m =Maximum adsorption capacity
q = amount adsorbed at equilibrium
c = concentration of free adsorptive at equilibrium
K = dissociation constant

A series of asumptions are made in the theoretical formulation of the Langmuir isotherm. It is assumed that only a fixed number of active sites are available for adsorption and a monolayer is formed through reversible adsorption. There are no lateral interactions between adsorbate molecules and all adsorption sites are identifical with no changes in the structure upon adsorption.

4.3. Adsorption Kinetics

To understand the mechanism of adsorption, it is also important to determine the mass transfer rates in a system. Determining the rate of adsorption is useful to know how fast the equilibrium phase is attained. The rate of adsorption is based on mass balances.

Analysis is based on finite rates of mass tranfer and an equilibrium isotherm or adsorption kinetics for a certain system.

Differences in rate theory models are mainly due to the differences in describing the mass transfer. Various steps (and resistances) to this mass transfer can exist:

1. Mass transfer from the fluid phase to the external surfaces of the adsorbent particles (film diffusion resistance)
2. Pore diffusion in the fluid phase (pore diffusion resistance)
3. Adsorption reaction at the phase boundaries (surface reaction resistance)
4. Diffusion in the sorbed state (particle phase diffusion resistance).

The rate limiting step may be one or a combination of the above mass transfer steps. For some adsorbents two mechanisms may occur in parallel and the faster controls the rate of adsorption. Each step involves a different concentration driving force and gives rise to a somewhat different form of mathematical result.

In the mathematical modelling of adsorption processes an option is to model a system as realistically as possible taking into account the individual resistances to mass transfer. However, the mathematics involved can be complex and in some circumstances an option may be to use simplified rate equations for the liquid-solid interface mass transfer, essentially combining the resistances to mass transfer to give what are known as lumped parameter models. These simplified models are used especially for well-stirred vessels when adsorbtion is homogeneous.

Experimental kinetic data are frequently analyzed with the Langmuir equation. The model assume that the adsorption can be taken as a reversible mass transfer process in which free adsorbate becomes bound to the adsorbent. The adsorption proceeds at a rate proportional to the product of the concentration of adsorbate in solution and the concentration of unused adsorbent. The reverse rate is proportional to the amount of adsorbate bound to the adsorbent. The rate equation describing the process can be written as:

$$\frac{dq}{dt} = K_a c(q_m - q) - K_d q \tag{4}$$

where c is the concentration of the adsorbate in solution and q is the concentration of adsorbate adsorbed on adsorbent. K_a and K_d are the forward and reverse rate coefficients and q_m is the maximum capacity of the adsorbent. $K = K_a / K_d$ is the dissociation constat. K_a and K_d include contributions from the individual resistances to mass transfer from the bulk of the mobile phase to the available sites on the adsorption media. K_a , K_d and q_m can be determined from equilibrium and mass transfer rate experiments. Adsorption equilibrium is attained when $dq/dt = 0$ and

$$K_a c(q_m - q) = K_d q \tag{5}$$

from this equality $q = \frac{q_m c}{K + c}$, where K is the dissociation constant.

4.4. Batch Adsorption

Batch adsorption is often used to adsorb solutes from liquid solutions when the quantities treated are small. An equilibrium relation such as Freundlich or Langmuir isotherm and a mass balance are needed. Initial feed concentration(c_0) and the final equilibrium concentration (c). q and qo are the final and initial concentrations on the adsorbent. W_s is the amount of adsorbent and V is the volume of feed solution.

$$c_0 V + q_0 W_s = cV + qW \tag{6}$$

This equation can be rearranged:

$$q = q_0 + \frac{V}{W_s}(c_0 - c) \tag{7}$$

If q is plotted against c according to the above equation, the result is a straight line. If the equilibrium isotherm is also plotted on the same graph, the intersection of both Iines gives the final equilibrium values of q and c.

When batch adsorption takes place in a well stirred vessel, concentration of the fluid in the vessel decreases with the progress of the process. In this case, the mass balance in the vessel will be expressed in the following form when $q_0 = 0$ is cosidered at t=0.

$$q = \frac{V}{W_s}(c_0 - c) \tag{8}$$

q can be calculated from the above equation. In the liquid phase adsorption, it is difficult to follow directly the change of amount adsorbed but the progress of adsorption may be traced by observing the concentration changes in the liquid phase as a function of time.

4.5. Protein Adsorption

Before protein adsorption behavior can be understood, it is first important to understand the basic makeup of protein structure. Proteins are complex copolymers that are made up of four levels of structure, designated as the primary, secondary, tertiary, and quaternary structures. The primary structure involves the specific sequence of the 20 L-amino acids coded for by the DNA of a cell. As part of a protein, a given amino acid is referred to as a peptide residue. Each amino acid, or residue, has the general backbone structure of f–NH– CaHR–CO–g, with R designating a specific side-group structure that gives the residue its specific functional characteristics. Accordingly, the amino acids are subcategorized into three primary types: nonpolar (i.e., hydrophobic), -charged, and polar. Examples of each type of amino acid are shown in Figure 4.2. (Latour 2005).

In the past decade, the researchers have conducted fundamental studies of the adsorption of acidic BSA, neutral MGB, and basic LSZ onto various kinds of synthetic HAp particles (Kandori, et al. 2007). Table 4.2. shows the properties of some proteins.

Table 4.2. Properties of proteins
(Source: Kandori, et al. 2007)

Proteins	Isoelectric point	Molecular weight (D_a)	Size (nm)	Numbers of functional groups (molecule^{-1})	
				$-NH_2$	-COOH
BSA	4.7	67,200	4×14	680	680
LSZ	11.1	14,600	3×3.5	155	32
MGB	7.0	17,800	3.5×4.5	34	36

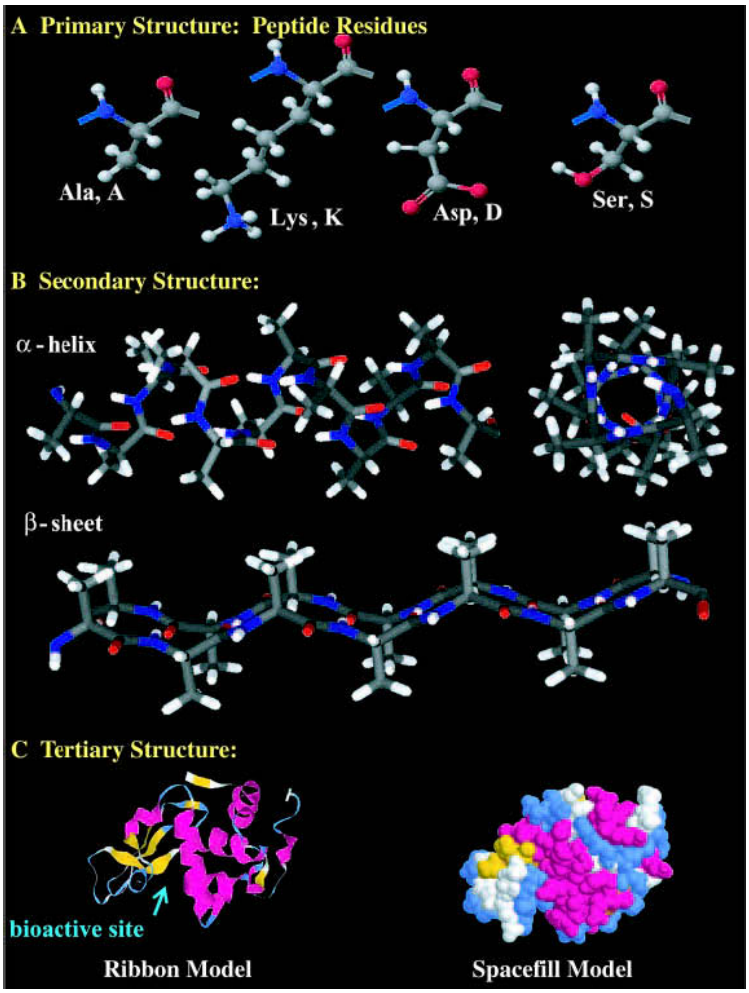

Figure 4.2. Protein structure

(Source: Latour 2005)

Albumin is the predominant plasma protein, making up 60–70% of plasma [20], yet it is not considered a mediator of acute inflammation. Although there is evidence that monocytes can and do, at least in vitro, adhere to albumin-coated surfaces, albumin is generally considered to "passivate" the surface and greatly reduce the acute inflammatory response to the material. Other constituents of plasma, despite their smaller numbers, must influence the adherence of phagocytic cells involved with inflammation (Zhoua, et al. 2007).

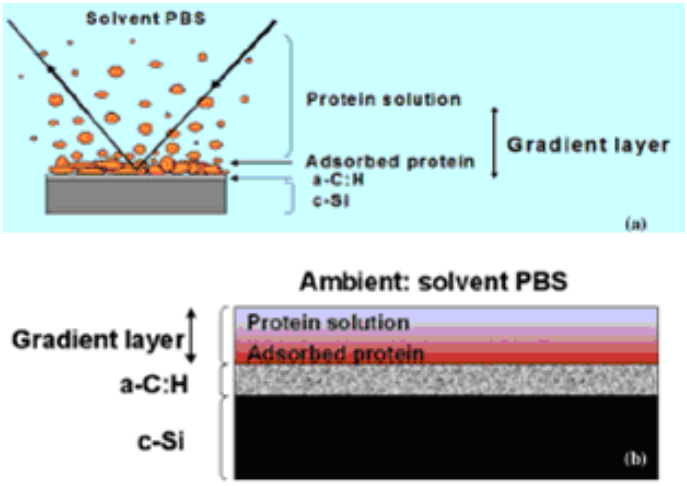

Figure 4.3. Protein Adsorption
(Source: Lousinian, et al. 2007)

Protein adsorption has been investigated extensively during the past decades. This is an important aspect for the improvement of many applications, such as medical implants, biosensor design, etc. When biomaterials are implanted into animals or humans, protein adsorption onto the foreign surface occurs within seconds of implantation (Kandori, et al. 2007). This rapid protein adsorption means that cells arriving at the biomaterial surface probably interact with the adsorbed protein layer rather than directly with the material itself. Thus, the initial protein adsorption onto a biomaterial surface plays a key role in how the body responds to an implanted biomaterial. Protein adsorption onto solid surface is given in Figure 4.3. (Lousinian, et al. 2007).

The density, orientation, and conformation of surface-bound proteins are believed to be key factors in controlling subsequent cellular adhesion (Lousinian, et al. 2007).

4.6. BSA Adsorption onto Chitosan, HA and Chitosan/ HA Composite Scaffolds

Protein adsorption characteristics of calcium hydroxyapatite modified with pyrophosphoric acids (PPa) were examined by Kandori, et al. (2007) The amounts of proteins adsorbed on the PP-Hap particles were measured by a batch method. This measurement was conducted at 15 $^{\circ}$C employing a 1×10^{-4} mol/dm^3 KCl solution of the protein in 10 cm^3 Nalgen polypropylene centrifugation tubes. The centrifugation tubes

were gently rotated end-over-end at 15 °C for 48 h in a thermostat. The amounts of adsorbed protein were measured by the microbiuret method using an UV absorption band at 310 nm after centrifuging the dispersions. Most of the UV experiments were triplicated and reproducible within 2%, indicating an uncertainty of 2×10^{-2} mg/m^2 for the amounts of protein adsorbed.

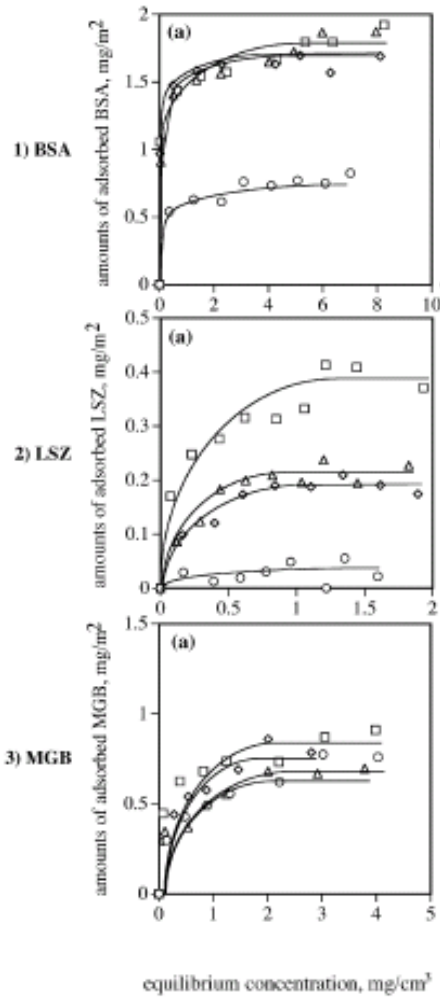

Figure 4.4. Adsorption isotherms of proteins. [PPa] mmol/dm^3 (o) unmodified, (◊) 2, (Δ) 4,and (□) 6
(Source: Kandori, et al. 2007)

The PPa modified HA particles (abbreviated as PP-HA) possessed anchored polyphosphate branches on their surfaces. The proteins of bovine serum albumin (BSA), myoglobin (MGB), and lysozyme (LSZ) were examined. The saturated amounts of adsorbed BSA were increased three-fold by the surface modification with PPa though

they were independent of the [PPa] as shown in Figure 4.4. This remarkable adsorption enhancement was explained by a three-dimensional binding mechanism. The anchored structure of the PP-branches developed on the HA surface to provide three-dimensional protein adsorption spaces was proved by a comparative experiment that was elucidating the effect of pyrophosphate ions for BSA adsorption onto HA.

Zhao, et al. (2007) fabricated two types of biomimetic composite materials, chitosan–gelatin (CG) and hydroxyapatite/chitosan–gelatin (HCG), and compared the effects of HA on human mesenchymal stem cell (hMSC) adhesion and 3-D construct development. Morphology of these composite materials are in Figure 4.5. The 2-D membranes were prepared to examine the influence of HA on adhesion efficiency of hMSCs, 3-D porous scaffolds were produced to investigate the effects of HA on material adsorption properties and 3-D hMSC construct development.

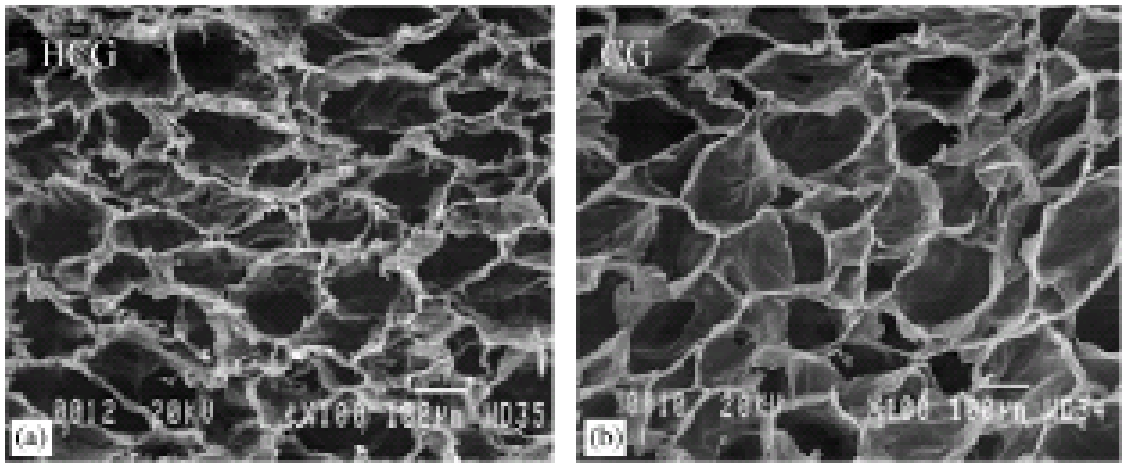

Figure 4.5. Morphology of the HCG (a) and CG (b) scaffolds
(Source: Zhao, et al. 2007)

After composite scaffolds were prepared by freeze-drying method, the 3-D porous HCG and CG scaffolds were treated with 50ml NaOH solution (10%) in 50ml ethanol followed by repeated washing with DI H_2O. The samples were put back into the freezer at -25 ^{0}C for 3 h and freeze-dried again in the lyophilizer at -60 ^{0}C for 12 h. The samples were weighed and then put into complete media for a predetermined time. The samples were taken out and washed with PBS three times for 5 min each, and then they were put back into the freezer at -25 ^{0}C for 3 h and freeze-dried again in the lyophilizer at -60 ^{0}C for 12 h. The samples were weighed and their weight changes were calculated

as average percentage increases of three samples. The media was changed every 3 days. The concentration of Ca^{2+} in the media was measured by Varian Spectra AA–640 Flame Atomic Absorption Spectrophotometer (FAAS). The concentration of the proteins in the media was quantified with a commercial protein assay kit (Bio-Rad Laboratories, Hercules, CA), using bovine serum albumin (BSA) standards. The concentrations of proteins and Ca^{2+} were the averages from three wells. The adsorbed calcium and proteins on the 3-D porous scaffolds were determined by subtracting the amount of calcium or proteins left in the media after adsorption from the amount of calcium or proteins in control media (without specimen) under the same incubation conditions.

The accumulated weights of proteins and calcium (Figure 4.6.) adsorbed on the 3-D porous scaffolds calculated from the concentration changes of proteins and Ca^{2+} in the media also revealed the adsorption characteristics of the materials. The adsorbed proteins and calcium increased with time on both 3-D HCG and CG scaffolds, and higher protein amount were detected in HCG, suggesting that the incorporation of HA in the scaffolds enhanced the protein and calcium adsorption capability of the scaffolds.

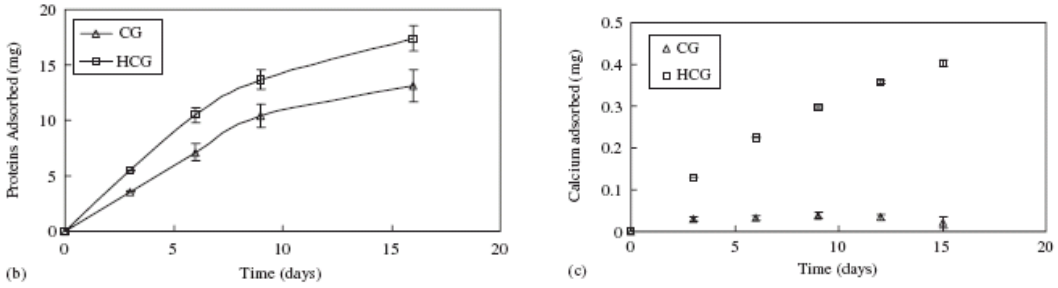

Figure 4.6. Absorption characteristics of 3-D HCG and CG scaffolds incubated in the complete media with 10% FBS as a function of time. (b) proteins adsorption on HCG and CG scaffolds; (c) calcium adsorption on HCG and CG scaffolds

(Source: Zhao, et al. 2007)

Figure 4.7. shows that the cells cultured in 3-D porous HCG scaffolds maintain significantly higher CFU-F numbers than the cells cultured in 3-D porous CG scaffolds during 35-day culture period, suggesting that hMSCs maintained higher differentiation potential in the HCG scaffolds.

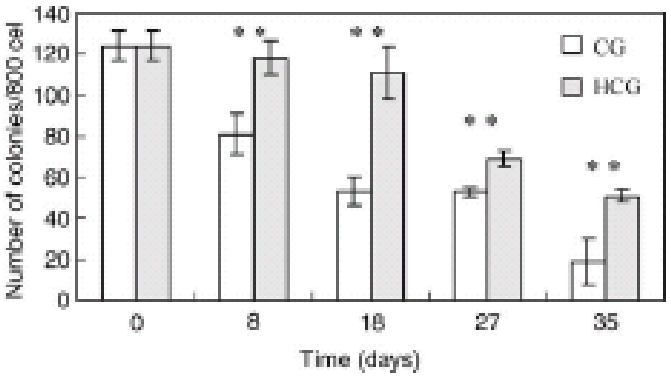

Figure 4.7. CFU-F levels of hMSCs cultured in HCG and CG scaffolds over a 35-day culture period
(Source: Zhao, et al. 2007)

In this study, HA was found to promote protein and calcium ion adsorption of the 3-D porous scaffolds in the complete tissue culture media. HMSCs exhibited higher initial cell adhesion efficiency to 2-D HCG membranes, and maintained higher proliferation rates in the 3-D porous HCG than CG scaffolds with 3.3 times higher final DNA amount in HCG scaffolds over a 35-day period. The results demonstrate that enhanced protein and calcium ion adsorption properties of HA in the CG polymer network improve initial cell adhesion and long-term growth, favor osteogenic differentiation upon induction, as well as maintain the progenicity of the 3-D hMSC constructs.

The adsorption characteristics of BSA onto the magnetic chitosan nanoparticles have been investigated by Wang, et al. (2001). They prepared the magnetic chitosan nanoparticles by adding the basic precipitant of NaOH solution into a W/O microemulsion system and observed the morphology of magnetic chitosan nanoparticles by transmission electron microscope (TEM). They found that the diameter of magnetic chitosan nanoparticles was from 10 nm to 20 nm, and the nanoparticles suspending in the aqueous solution could easily aggregate by a magnet, which suggested that the nanoparticles had good magnetic characteristics.

Three milligrams of magnetic chitosan nanoparticles and 3 ml of BSA buffer phosphate acid solution were added into a 5 ml of centrifugal tube, the mixture was stirred for 30 min, the nanoparticles were precipitated with centrifugation (10,000 rpm for 7 min). The upper clear liquid was obtained and the BSA concentration was

measured with the Folin method. Changing the initial BSA concentration and pH of BSA solution, the equilibrium was investigated. When the adsorption kinetics was measured, 10 μL of samples were taken every certain time. The adsorption capacity under different pH was investigated. Under the comprehensive function of many factors, the highest adsorption capacity of BSA is achieved at pH=4. The adsorption loading reaches the maximum 110 mg/g when the pH of solution is equal to 4. Because the diameter of magnetic chitosan nanoparticles is between 10 and 20 nm, and then the composite nanoparticles have larger surface-to-volume ratios, more functional groups are exposed. So the magnetic chitosan nanoparticles have larger capacity.

Using 3 mg of magnetic chitosan nanoparticles adsorbed 3 ml of BSA solution with initial concentration of 300 mg/l, the adsorption kinetics is studied. Since the nanoparticle has very small diameter and great surface-to-volume ratio, it can quickly reach the adsorption equilibrium. Within 10 min it achieved the adsorption equilibrium.

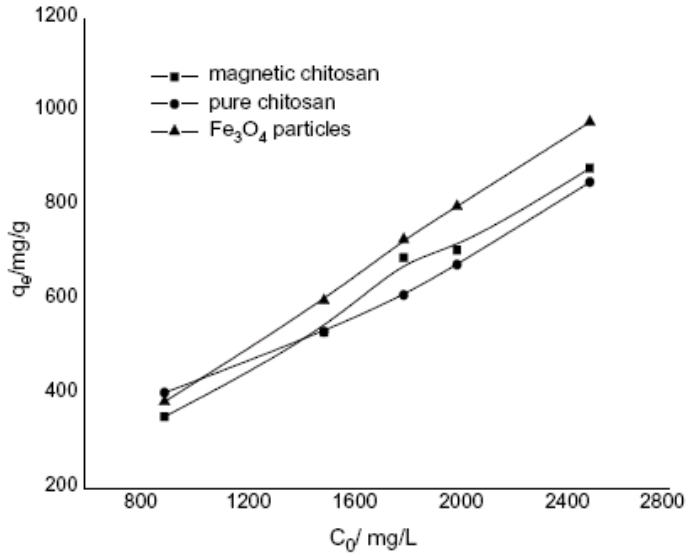

Figure 4.8. Comparison of the adsorption loading of chitosan nanoparticles, Fe_3O_4 nanoparticles and the composite nanoparticles
(Source: Wang, et al. 2001)

Figure 4.8. shows the adsorption capacity of chitosan nanoparticles, magnetic chitosan nanoparticles and Fe_3O_4 nanoparticles. It was found that the adsorption capacity of composite chitosan nanoparticles was a little higher than that of pure chitosan, this is because the Fe_3O_4 is also available to adsorb many BSA, the NH_2 group

of BSA molecule can bind with the orbit of Fe atom, the capacity of Fe_3O_4 nanoparticles which was obtained by calcining the composite nanoparticles to remove the chitosan was higher than that of pure chitosan nanoparticles.

In this study, the BSA adsorption experiment indicated that when pH of BSA solution was equal to 4, the maximum adsorption loading reached 110 mg/g. Through measuring the zeta potential of BSA solution and the magnetic nanoparticles, it was found that under this situation the surface of BSA took the negative charge, but the magnetic nanoparticles took the positive charge. Due to the small diameter, the adsorption equilibrium of BSA onto the nanoparticles reached very quickly within 10 min. The experimental results showed that the magnetic chitosan nanoparticles have potential to be used for the quick pretreatment in the protein analysis process.

Hoven, et al. (2007) investigated protein adsorption characteristics of positively charged chitosan film (QAC film) and negatively charged chitosan film (SFC film). Protein solutions were freshly prepared by dissolving albumin, fibrinogen, lysozyme and ribonuclease in PBS at pH=7.4 to give a final concentration of 1 mg/ml. To reach an equilibrium hydration, the film substrate was immersed in the PBS solution overnight prior to adsorption. Each sample was removed from PBS solution and suspended into the wells containing 3 ml protein solution before incubation at 37 ^{0}C for 3 h. Then the films were removed and rinsed with 4x10 ml PBS solution to remove reversibly adsorbed protein. To remove irreversibly adsorbed protein from the film surface, each film was transferred to another vial containing 2.0 ml of 1.0 wt% sodium dodecyl sulfate (SDS) and soaked for 1 h at room temperature. To determine the total amount of protein adsorbed on the substrates, Bicinchoninic acid (BCA) protein assay was utilized. The absorbance of the solution was measured at 562 nm by UV-VIS spectroscopy (Microtiter plate reader; model Sunrise, Tecan Austria GmbH). The amount of adsorbed protein was determined by comparison of the absorbance of the samples with a calibration curve. Three repetitions were performed for all samples. With respect to chitosan films, the adsorbed amounts of all proteins on SFC films are shown in Figure 4.9.

The proteins used in this investigation include albumin (BSA), fibrinogen (FIB), ribonuclease (RNase), and lysozyme (LYZ). BSA and FIB were selected as models of negatively charged proteins, whereas RNase and LYZ represent proteins carrying a positive charge. The protein concentration of 1 mg/ml used in adsorption studies is in the plateau region of the adsorption isotherm determined for all four proteins.

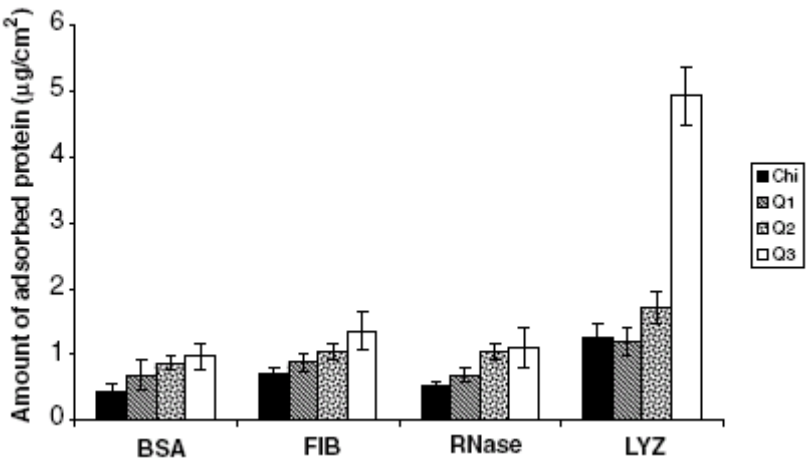

Figure 4.9. Amount of adsorbed proteins on QAC films in comparison with chitosan films

(Source: Hoven, et al. 2007)

CHAPTER 5

EXPERIMENTAL

5.1. Materials

Polymeric material used in this study was low molecular weight chitosan and commercial hydroxyapatite purchased from Sigma-Aldrich. Acetic acid (glacial), purchased from Merck, was used as a solvent after dilution by deionised water, for the preparation of the polymer solution. Properties of materials used for the production of scaffolds are given in Table 5.1. Protein used was Bovine Serum Albumin (BSA) from Sigma. Properties of BSA are given in Table 5.2.

Table 5.1. Properties of Materials Used in This Study

	Hydroxyapatite	**Acetic Acid**	**Chitosan**
Chemical Formula	$Ca_{10}(PO_4)_6(OH)_2$	CH_3COOH	---
Molecular weight (g/mol)	1004.6	60.05	---
Density (g/cm^3)	3.14	1.05	1.51

Table 5.2. Properties of Bovine Serum Albumin

Molecular weight (g/mol)	66.700
Dimensions (nm)	4x4x14
Density (g/cm^3)	1.36
Isoelectric point (pI) pH	4.7-4.9

Human Serum Protein (HSP) used for the adsorption studies was collected from blood serum of 5 healty volunteers. The serum protein amount was measured as 680mg/ml and stored in the freezer at -20 ^{0}C for stock protein solution.

Buffer solutions prepared for the adsorption experiments were as follows:

- 0.2 M monobasic sodium phosphate stock solution (13.9 g $NaH_2PO_4.H_2O$ was dissolved in deionized water and diluted to 500 ml).

- 0.2 M dibasic sodium phosphate stock solution (14.2 g Na_2HPO_4 was dissolved in deionized water and diluted to 500 ml).

- 10 mM Sodium phosphate buffer solution (PBS) (34.5 ml dibasic stock solution and 15.5 ml monobasic stock solution were mixed and diluted to 1000 ml with deionized water) for pH=7.4.

- 10 mM Sodium phosphate buffer solution (PBS) (2 ml dibasic stock solution and 48 mlmonobasic stock solution were mixed and diluted to 1000 ml with deionized water) for pH= 5.7.

- Simulated body fluid (SBF) was prepared by dissolving the reagent grade chemicals through the addition of the respective amounts in the following order: NaCl, $NaHCO_3$, KCl, Na_2HPO_4, $MgCl_2.6H_2O$, $CaCl_2$, and $NaSO_4$ in deionized water.The composition of SBF and plasma are given in Table 5.3. The solution was buffered at physiological pH of 7.4 at 37^0C with 50 mM trishydoximethyl aminomethane [$(CH_2OH)_3$ (CNH_2)] (THAM) and 36.23 mM of HCl acid. Most of the HCl was added before the $CaCl_2$ addition and the pH was adjusted with HCl acid after THAM addition.

Table 5.3. Ion concentrations (mM) of simulated body fluid (SBF) and human blood plasma

	Na^+	K^+	Ca^{2+}	Mg^{2+}	Cl^-	HCO_3^-	HPO_4^-	SO_4^-	buffer
Plasma	142	5.0	2.5	1.5	103	27	1.0	0.5	-
SBF	142	5.0	2.5	1.5	125	27	1.0	0.5	THAM

5.2. Methods

5.2.1. Freeze- Drying Method for Porous Chitosan/ HA Production

The chitosan/hydroxyapatite composites were coded as C100H0 to C20H80. The composites and their compositions are in Table 5.4.

Table 5.4. wt % of hydroxyapatite and chitosan in Chitosan/ HA composites

SAMPLE	wt %	
	HA	CHITOSAN
C100H0	0	100
C80H20	20	80
C70H30	30	70
C50H50	50	50
C30H70	70	30
C20H80	80	20

Acetic acid was used as the solvent to prepare the polymer solutions. By using 2 v/v % acetic acid solution, chitosan was dissolved by using magnetic stirrer for 3h and the polymer solution was left overnight at room temperature to remove the air bubbles trapped in the viscous solution. Then predetermined amount of hydroxyapatite was dispersed in deionised water by 30 min ultrasonic treatment. Ultrasonic treatment was necessary to avoid agglomeration of ceramic powder and to achieve proper dispersion. Hydroxyapatite in water was mixed with polymer solution under agitation. In all the samples chitosan amount was fixed and hydroxyapatite amount was changed. The homogeneously mixed solution was poured in a syrnge which was used as cylindrical moulds and immediately taken to deep freeze at –20 ^{o}C and –80 ^{o}C. After 24 h freezing the samples were quickly placed into the freeze drier (Labconco) containers and freeze dried for 30-36 hours. A picture of the freeze drier used in this work is shown in Figure 5.1.

Figure 5.1. The picture of LABCONCO Freeze Dryer used for the preparation of composites in this work

The freeze dried composites were further dried at 35^{o}C for 48h. Finally the samples were cut into discs and used for SEM and protein adsorption measurements.

5.2.2. Characterization of Composites

Scanning Electron Microscopy (SEM) (Philips XL 30SFEG) was used to determine the morphology of the composites. The porosities and densities of the composites were determined by determining their dimensions and weight. The density of of the starting chitosan powder was determined by using Helium pycnometer. Weight loss curve of scaffolds were determined by thermogravimetric analysis (TGA) using a Shimadzu TGA-51 instrument with a constant heating rate of 4 ^{0}C /min up to 1000 ^{0}C under a dry N_2 stream. Differential Scanning Calorimetry (DSC Shimadzu) and Fourier Transform Infrared Spectrophotometer (FTIR Shimadzu 8201) analysis were also carried out.

5.2.3. Adsorption Studies and Bradford Method for Determination of Adsorbed BSA

Protein solutions were freshly prepared by dissolving albumin in PBS at pH=7.4 and 5.7 to give a final concentration of 1 mg/ml. Scaffolds (40 mg) were soaked in 100

% ethanol for an hour and in phosphate buffer solution (PBS) for 30 min twice. Each sample was removed from PBS solution and suspended in the tubes containing 5 ml protein solution and incubated at 37 ^{0}C for 3 h. In some experiments concentration of BSA solution was fixed and different scaffold samples were used for the adsorption studies. Other experiments were carried out with various BSA concentrations (0.1- 1 mg/ml) using the same sample. The adsorption was conducted under constant temperature of 37 ◦C for 3 hours in a thermal shaker at 150 rpm. Then the scaffolds were centrifuged and the supernatant was saved for protein concentration determination. The amount of protein in the supernatant was quantified by the absorbance at 595 and 280 nm using a UV spectrophotometer. The amount of adsorbed protein was determined by comparison of the absorbance of the samples with a calibration curve.

The wetted scaffolds were incubated in bovine serum albumin solutions for 3 h on the shaker (150 rpm). After the 3 h incubation period, the scaffold was removed from the protein solution The remaining proteins in the solution was measured using Bradford protein assay at 595 nm or absorbance assay at 280 nm in quartz cuvettes.

Absorbance assay at 280 nm was fast and convenient, since no additional reagents or incubations were required. Proteins in solution absorb UV light with absorbance maximum at 280 nm. Amino acids with aromatic rings are the primary reason for the absorbance peak at 280 nm.

Bradford protein assay depends on the prencibles of complexing Coomassie Brillant Blue with proteins to give an absoption maximum at 595 nm. It is a simple method with colour developing rapidly to produce a stable complex and is sensitive dawn to 40 µg protein per ml. Bradford's solution was prepared by dissolving 100 mg Coomassie Brillant Blue G-250 in 50 ml ethanol (95 %) , adding 100 ml of phosphoric acid (85 % w/v) and diluting to 1 liter with deionized water, respectively. Solution was filtered through the filter paper into a dark bottle and stored at +4 ^{o}C. For absorbance measurement, spectrophotometer was switch on and allowed to warm up at least 15 min. 1000 µL sample and the 1000 µL of the dye reagent accurately pipetted, fixed in the vortex and incubated for 15 min at room temperature. Absorbance was measured at 595 nm. The concentration of sample was obtained from a standard curve obtained by using known concentrations of standard protein (BSA).

Standard calibration curve obtained by using BSA protein standard (Sigma) was plotted using Bradford protein assay. Standard curve was obtained by using bovine serum albumin solutions (BSA) with concentrations of 0, 4, 10, 20, 30, 40 µg/ml for the

standard assay. After carried out Bradford Protein Assay procedure absorbance of these concentrations were measured at 595 nm. A calibration curve was prepared by plotting the absorbance values of the standarts versus their corresponding protein concentrations. These protein concentrations were further multiplied with the dilution factors in order to obtain the actual protein concentrations in the orginal sample (c). Calibration curve at 280 nm was also plotted with the BSA protein standard. Using these standard curves the concentration for an unknown sample was estimated at the given absorbance reading. These three calibration curves (BSA at 595 and 280 nm, and HSP at 280 nm) are given in the Appendix.

After BSA equilibrium concentrations were determined, the amount of BSA adsorbed on scaffolds was calculated from the following equation:

$$q = \frac{V}{W_s}(c_0 - c) \tag{9}$$

Where c_o is the initial BSA concentration in the solution, c is the equilibrium BSA concentration, V is the sample volume, and the W_s is the amount of composite scaffold used. Adsorption isotherms were obtained for each pH value plotting q(amount of BSA adsorbed on scaffold, mg BSA/g sample) versus equilibrium concentration of BSA (c) in the solution.

Batch kinetic experiments were carried out to determine the amount of BSA adsorbed on scaffolds against time. 40 mg composite scaffold was added to 5 ml protein solution with identical experimental conditions with adsorption isotherm determinations. Samples from the tubes were taken out at certain time intervals, a similar procedure was followed as described earlier in adsorption isotherm experiments and q versus t plots were prepared.

CHAPTER 6

RESULTS AND DISCUSSION

In this study the preparation, characterization and protein adsorption behaviour of porous hydroxyapatite/chitosan scaffolds were investigated. The effects of processing parameters like the HA/chitosan ratio and pH on protein adsorption onto HA/chitosan composite biomaterials were examined and discussed. The difficulties in the UV based absorbance measurement methods at 595 and 280 nm for the protein (BSA and HSP) concentration determination, the reliability and reproducibility of this data together with the degradation tendency of freeze-dried chitosan have been discussed and reported.

6.1. Characterization of Porous Hydroxyapatite /Chitosan composites

The physical, microstructural and thermal properties of chitosan / HA composite scaffold biomaterials varies with the increasing HA content. The estimated theoretical densities (from the theoretical densities of the pure components HA and chitosan 3.16 and 1.52g/cc respectively), the bulk densities from dimensions and weights of composite samples.

As can be seen in Table 6.1. and Figure 6.1. when chitosan amount decreased and hydroxyapatite content increased the density of the composite increased which led to a decrease in porosity. C20H80 had the lowest porosity and highest density while C100H0 had the lowest density and highest porosity. The composites had porosities in the 93.5-96.25 % range where the density of the freeze-dried pure chitosan scaffold had the lowest density of 0.057 g/cc. Since the total volume of the frozen polymer/HA dispersions were kept approximately constant at about 40 ml, the density of the freeze-dried composites increased as the HA content increased. There seems to a relatively faster change in the porosity level in the 30-60% Chitosan composites as seen in Figure 6.1.

Table 6.1. Densities of HA/Chitosan composites

TD	% Chitosan	density	% of TD	% porosity
2.604	20	0.17	6.53	93.47
2.392	30	0.148	6.19	93.81
2.053	50	0.106	5.16	94.84
1.923	60	0.0875	4.55	95.45
1.802	70	0.074	4.11	95.89
1.696	80	0.067	3.95	96.05
1.52	100	0.057	3.75	96.25

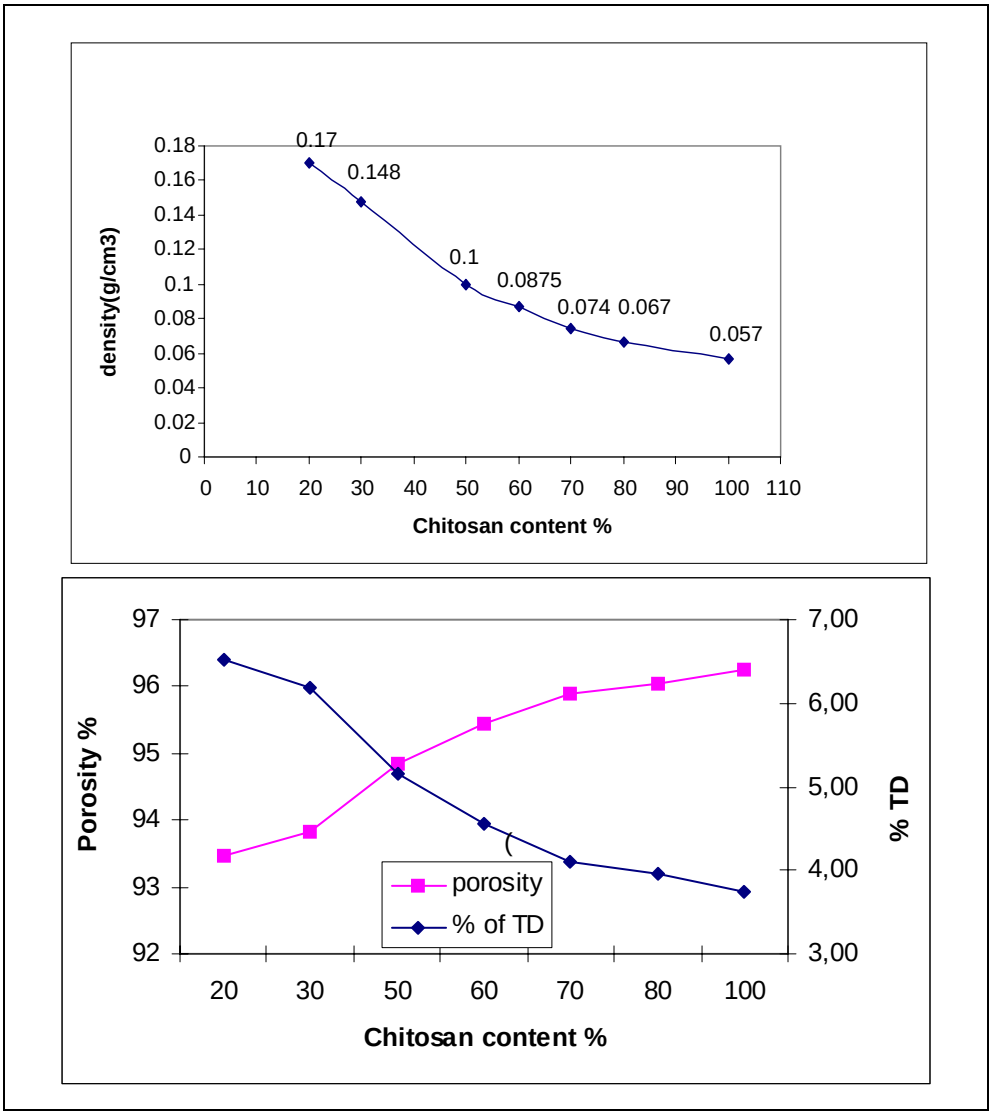

Figure 6.1. The variation of density and porosity of the chitosan composites with composition

The SEM images of the hydroxyapatite/chitosan composites are given in Figures 6.2. through 6.7. When all the SEM images of composites are considered highly porous structure was common in all these materials. The smoothest surface at pure chitosan began to be disturbed with incorporation of hydroxyapatite gradually resulting in a rough surface which was not smooth anymore. The HA particles were embedded well in the chitosan matrix. The pore sizes were around 50–250 μ.

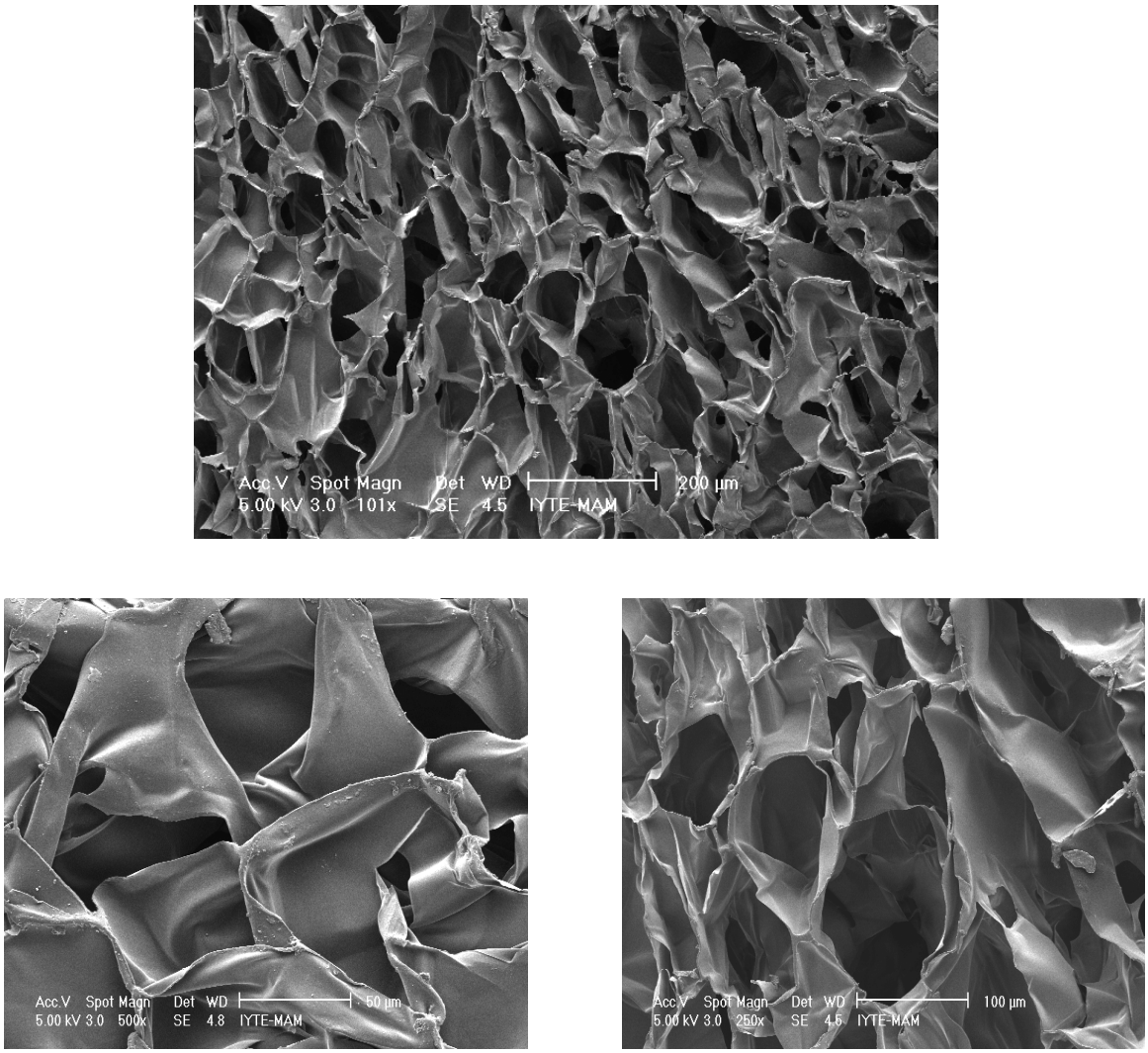

Figure 6.2. Scanning electron (SEM) micrographs of C100H0 composites frozen at -20 ^{0}C before freeze drying

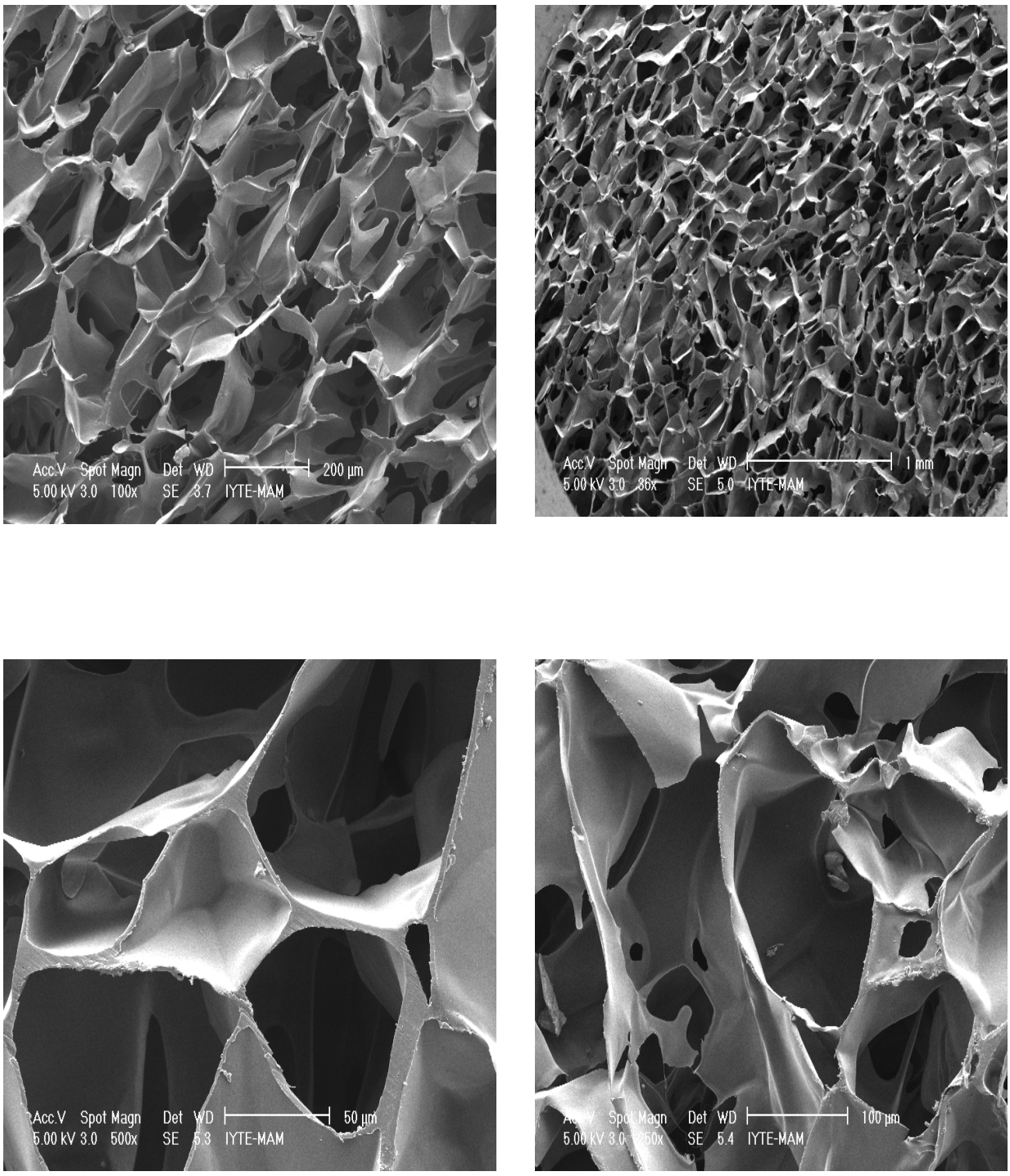

Figure 6.3. Scanning electron (SEM) micrographs of C100H0 composites frozen at -80 ^{0}C before freeze drying

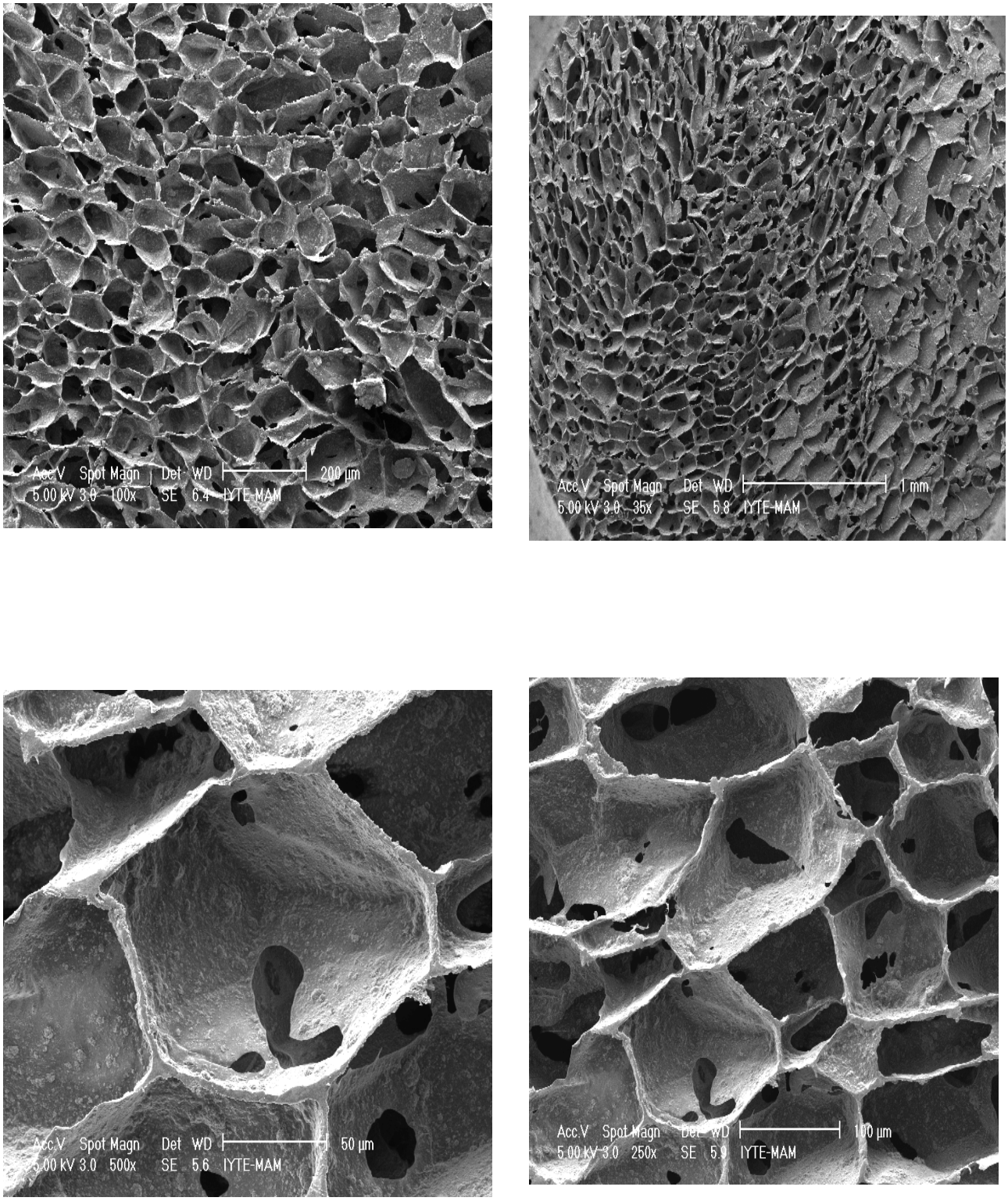

Figure 6.4. Scanning electron (SEM) micrographs of C50H50 composites frozen at -20 ^{0}C before freeze drying

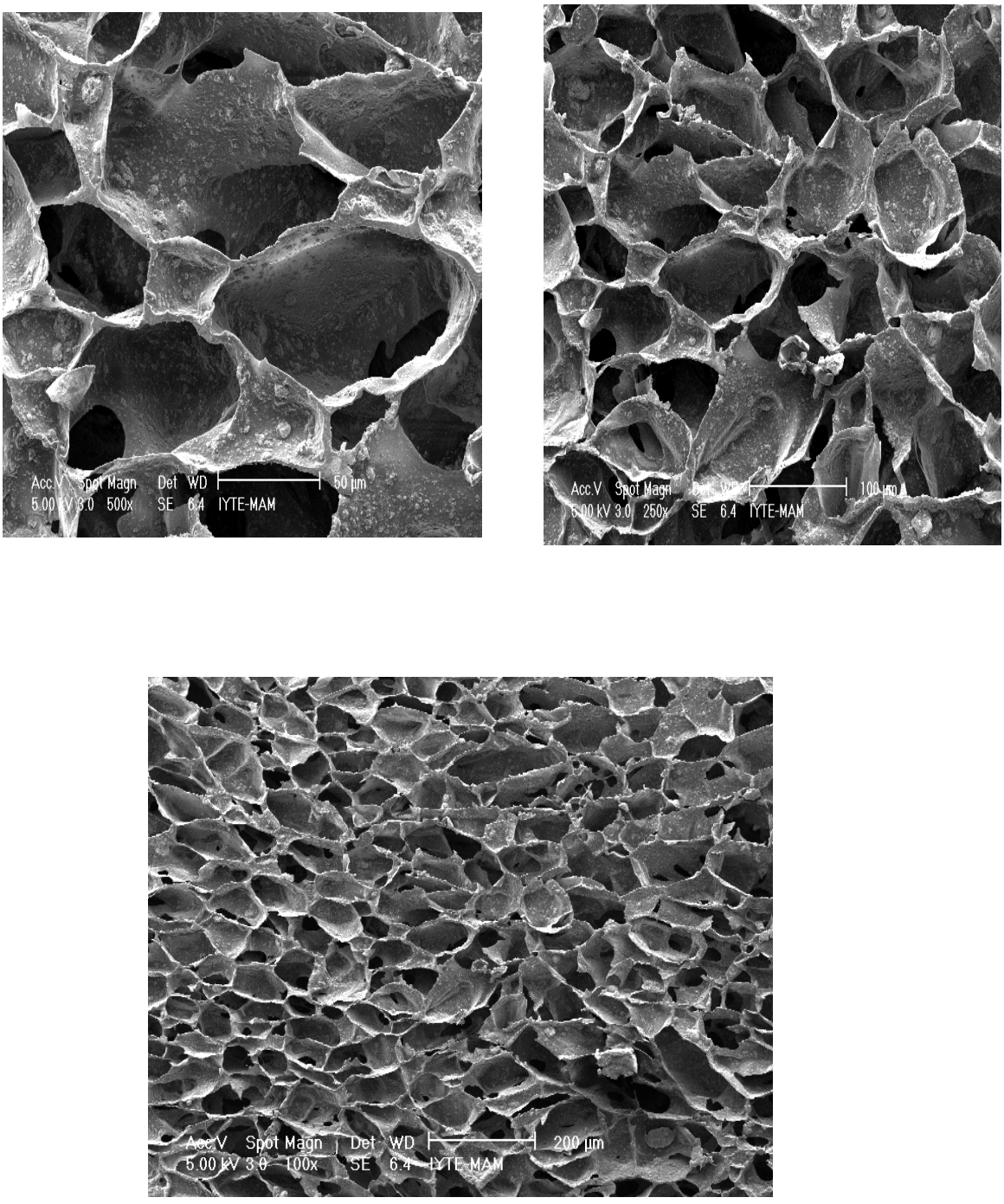

Figure 6.5. Scanning electron (SEM) micrographs of C50H50 compositesfrozen at -80 ^{0}C before freeze drying

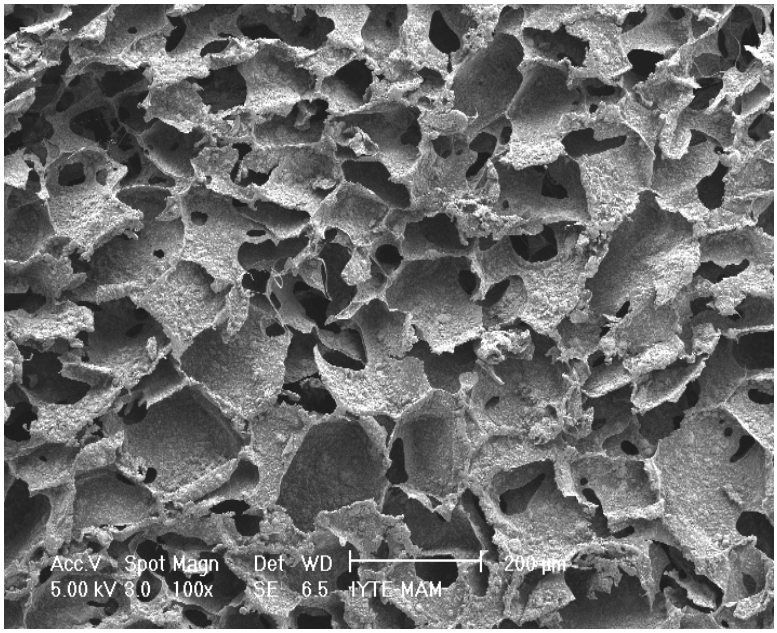

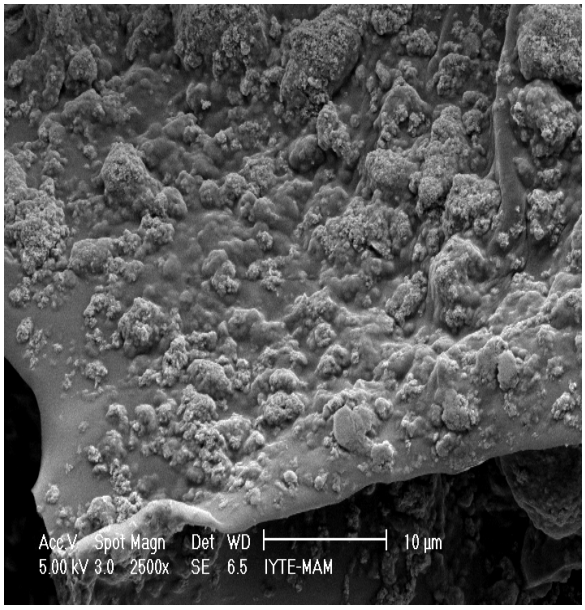

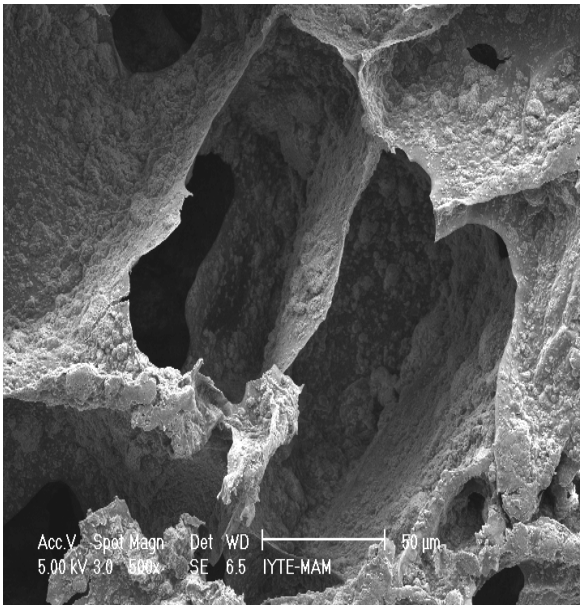

Figure 6.6. Scanning electron (SEM) micrographs of C30H70 composites frozen at -20 ^{0}C before freeze drying

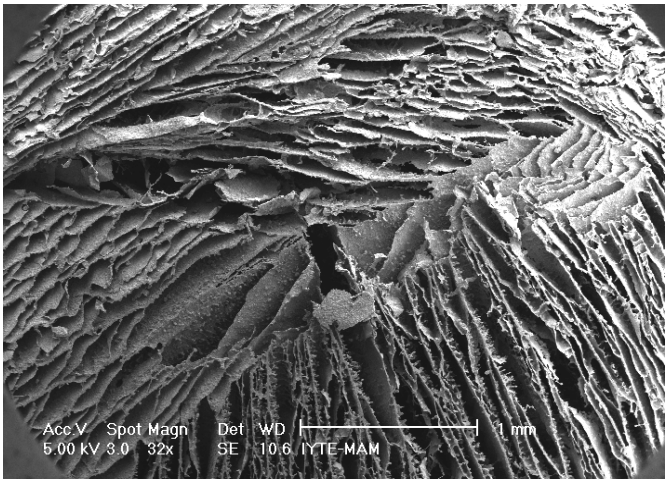

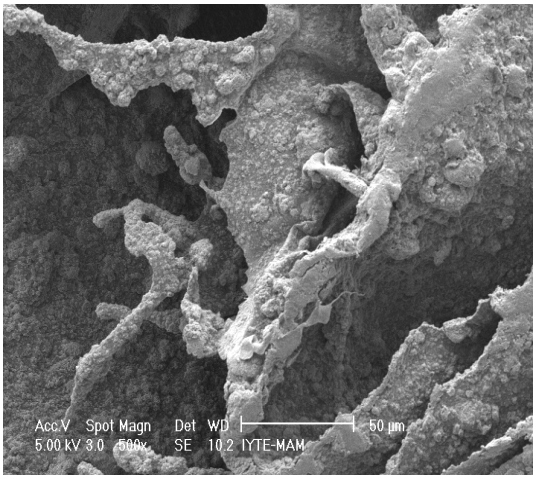

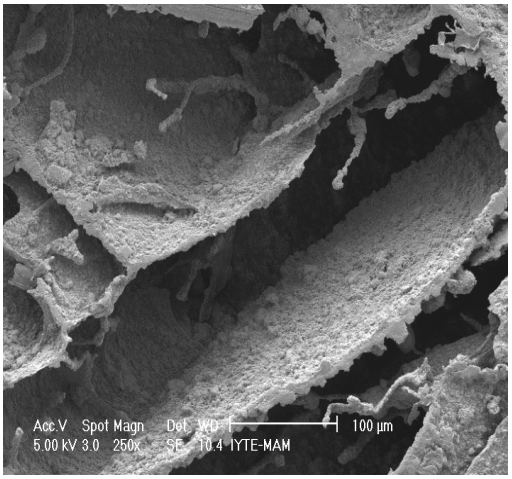

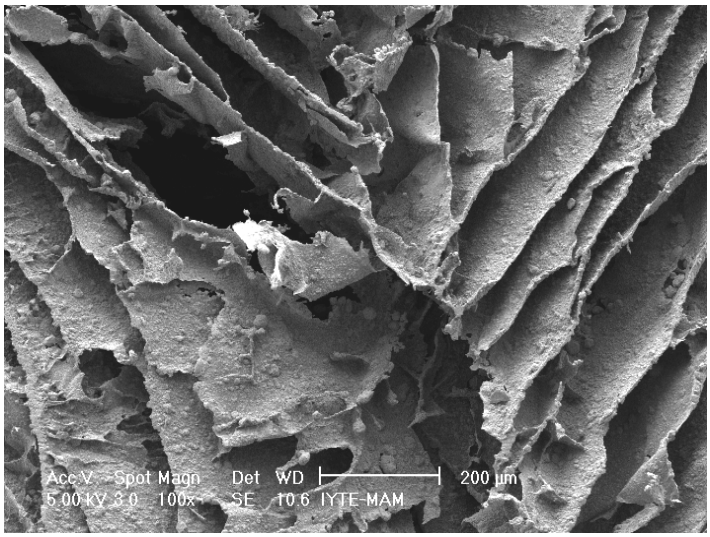

Figure 6.7. Scanning electron (SEM) micrographs of C30H70 composites frozen at -80 ^{0}C before freeze drying

Increasing hydroxyapatite content did not disturb the porous structure exceptally some C30H70 70wt HA, the effect of HA on the morphology was significant. The pores decreased in size, cavities between cells became thin, uniformity decreased and surface became rough, in some samples lameller structure was observed.

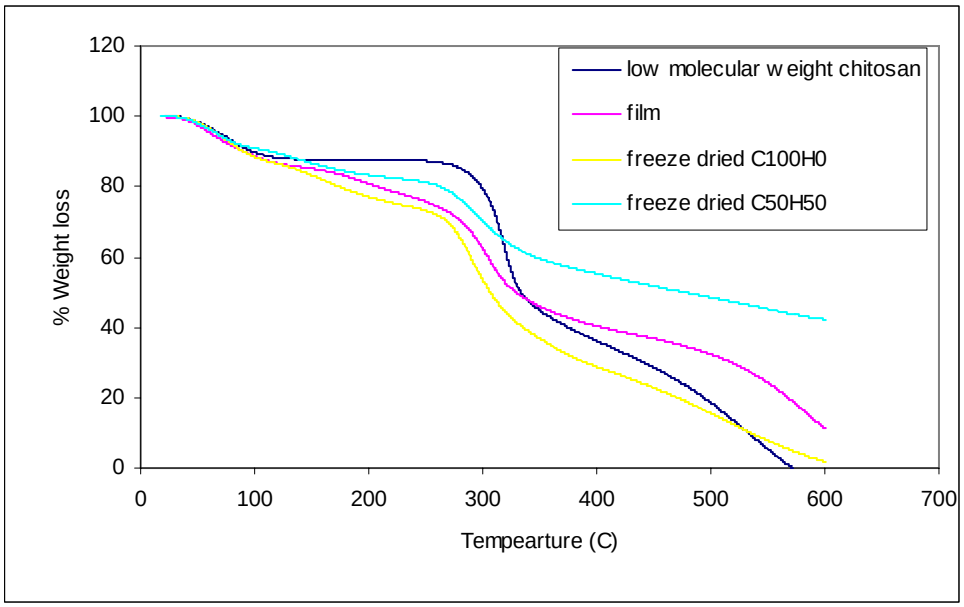

Figure 6.8. The Thermogravimetry (TGA) curves for low molecular weight raw chitosan, C100H0, C50H50 and chitosan film

The TGA curves of the raw unprocessed low molecular weight chitosan along with two composites (C100H0 and C50H50) and the film prepared by room temperateure drying of chitosan-acetic acid clear solution is given in Figure 6.8. The DSC curves of low and medium molecular weight chitosan, the same composites and the film are given in Figures 6.9. through 6.11.There is an initial weight loss of about 10-15% in all TGA curves up to 100-150^{o}C in all four samples which most likely is due to the removal of water from the structures. This was in good aggreement with the endothermic low temperature peaks observed below 100^{o}C in all DC curves. Significant differences in the TGA curves in the 150-300^{o}C range were observed as seen in Figure 6.8. Although there was a temperature range (approximately 150-280^{o}C) with almost no weight loss in the TGA curve of unprocessed raw low molecular weight chitosan, in the same internal there were significant weight losses in all the other TGA curves. This indicates that the structure changes upon dissolution in the acetic acid

solution and freeze drying and becomes less ordered and easier to degrade upon heating in that range. The relatively sharp weight loss curve becomes wider.

The steep exothermic peaks observed in all DSC curves at about 290-310^{o}C is in aggreement with the TGA behaviour and was most likely due to thermal degradation of the biopolymer. There are extra peaks located at about 240^{o}C for the two freeze-dried composites. The reason for their presence may be related to the removal of acetic acid/acetyl groups from the porous/high surface area polymeric matrix relatively easy at that lower temperature range.

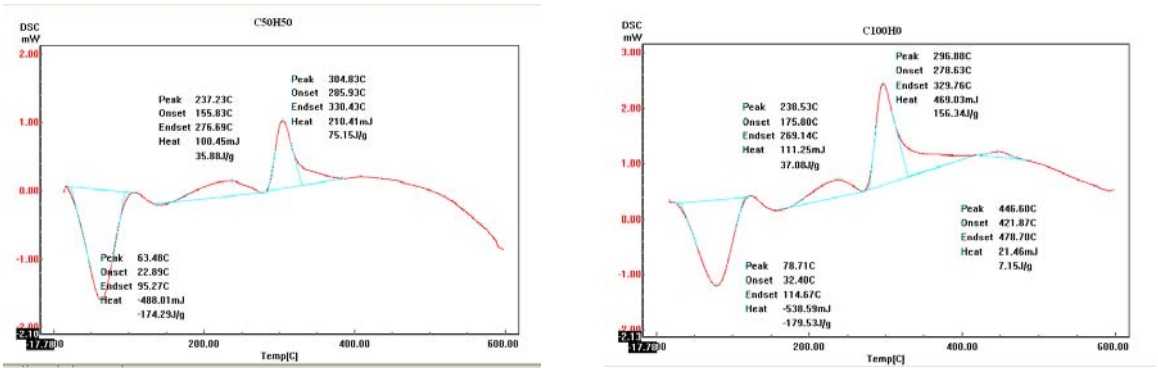

Figure 6.9. Differential Scanning Calorimeter (DSC) curvesfor C100H0 and C50H50 chitosan composites

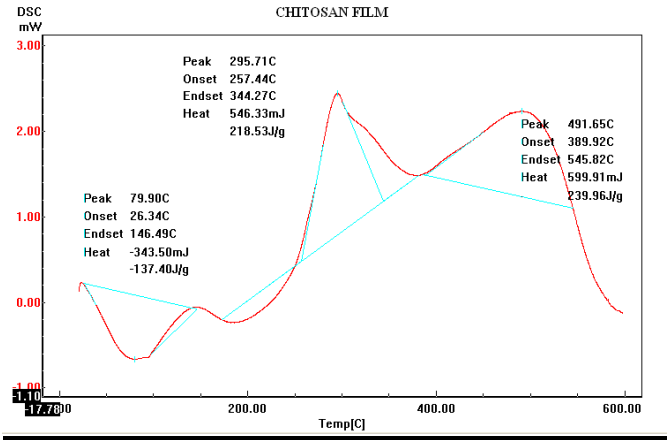

Figure 6.10. Differential Scanning Calorimeter (DSC) curves for Chitosan film

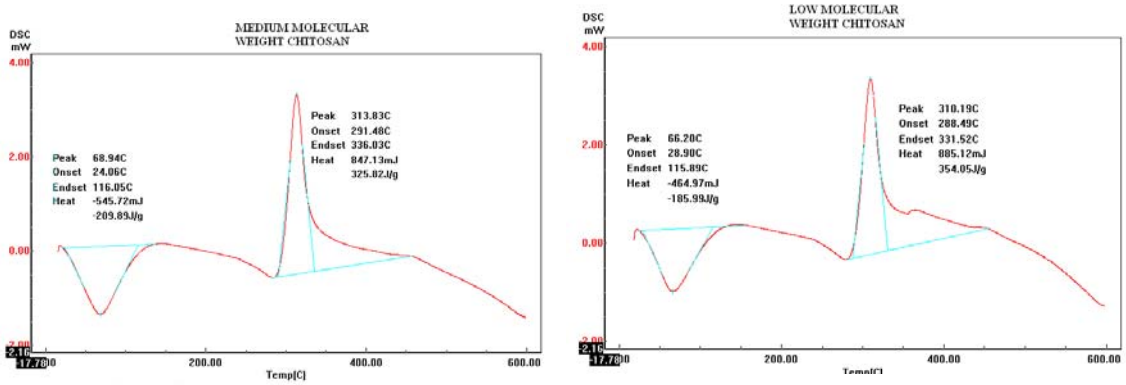

Figure 6.11. Differential Scanning Calorimeter (DSC) curves for medium and low molecular weight Chitosan film

6.2. Adsorption of BSA onto Chitosan/HA Composite Scaffolds

Uptake of BSA by chitosan/HA composite (C50H50) at time scale for two pH values are given in Figures 6.12-6.14. The effect of pH on uptake profiles at a fixed initial BSA concentration (C_0=1 mg/ml) have been investigated by using 280 and 595 nm UV-based concentration determination methods. The presence of an initial rapid adsorption period (which was approximately in the 120-180 minutes range) is evident in all the three plots where more than 75% of the total adsorption takes place. For the C50H50 composite (determined to be 95% porous) the maximum BSA uptake levels were about 80 mg/g composite and was independent of pH and UV method. It was assumed that adsorption equilibrium was achieved in 3 hours in the rest of this work based on this observation.

The freeze dried pure chitosan and chitosan/HA composites were observed to swell considerably upon soaking in aqueous solutions thus a large amount of solution is enclosed in the gel-like swollen composite structure. This necessitated the common application in earlier work by other researchers the NaOH (through the neutralization of the surface acidic functional groups) and ethanol soaking pretreatments (Zhao, et al. 2000) or copolymerization of the starting biopolymer in order to stabilize the structure. Since chitosan is a biodegradable polymer, the influence of its degradation/swelling tendency/unstability on the protein adsorption equilibrium was investigated by soaking the C50H50 composite in the pH=5.7 buffer and following the absorbance of the

supernatant by the Bradford method at 595 nm as a function of time. The result of this work is given as % of original soaked composite dissolved in the buffer as a fuction of time in Figure 6.15. The presence of a rapid initial dissolution stage of chitosan in the first two hours of soaking in the pH=5.7 buffer accounting for almost about 5wt% dissolution of the original composite is evident in Figure 6.15. The dissolution level somewhat stabilized in the 5-7 wt% range for up to 24 h of soaking. The raw chitosan (RC) was dissolved in acetic acid solution similarly to the composite preparation and a standard calibration curve (similar to the standard calibration curves for BSA and HSP given in the Appendix) was obtained with the Bradford method at 595 nm and is given in Figure 6.16. This was done in order to see whether dissolved chitosan reacted with the dye used in the Bradford method and caused absorbance during the concentration determination. Although the dissolution of chitosan was quantified the calibration curve leveled of, which for accurate determination must diplay a linear relation between the absorbance and the concentration. Due to the presence of dissolution and interference from the chitosan present in the solution, blank chitosan samples were soaked in the respective media and the absorbance values were corrected with these blank values in the rest of this work for accurate protein concentration determination in the supernatants.

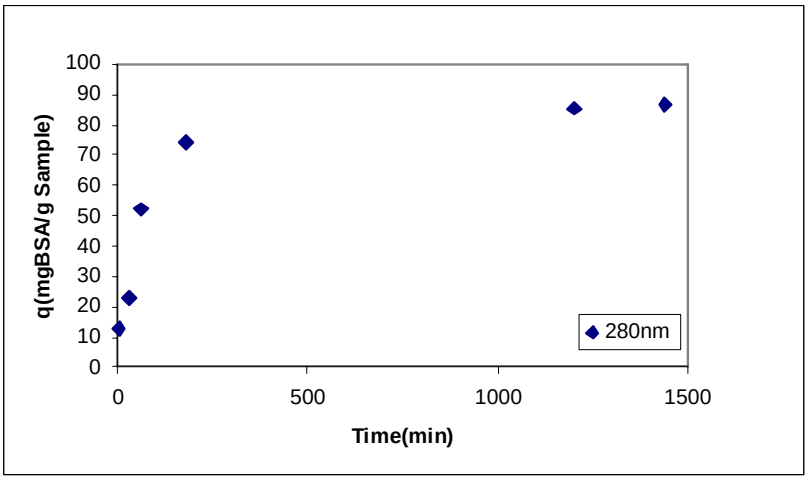

Figure 6.12. Uptake of BSA by C50H50 at pH=7.4

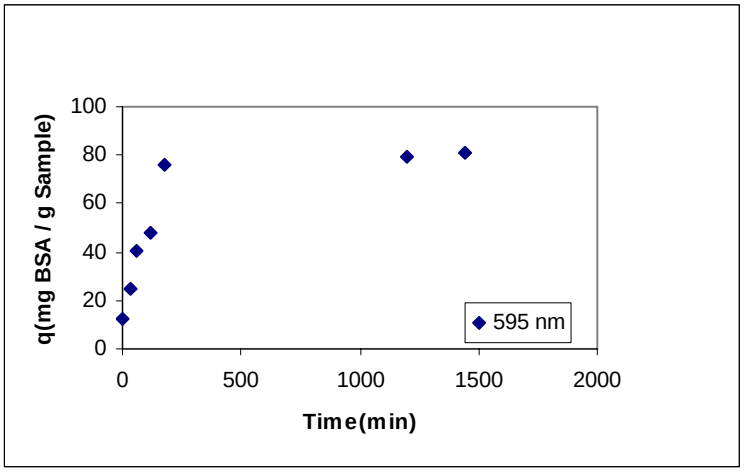

Figure 6.13. Uptake of BSA by C50H50 at pH=7.4

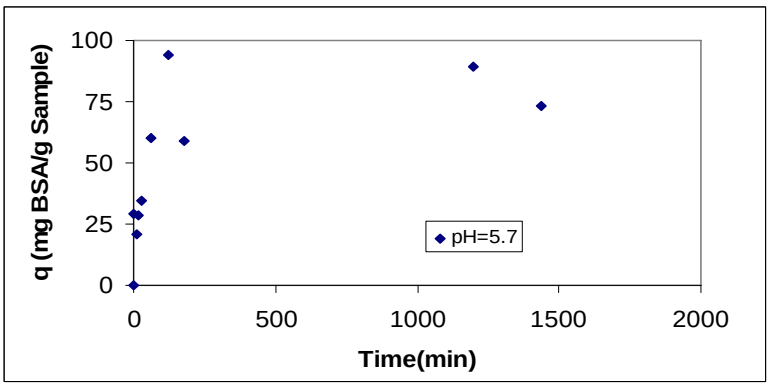

Figure 6.14. Uptake of BSA by C50H50 at pH=5.7 and 595 nm

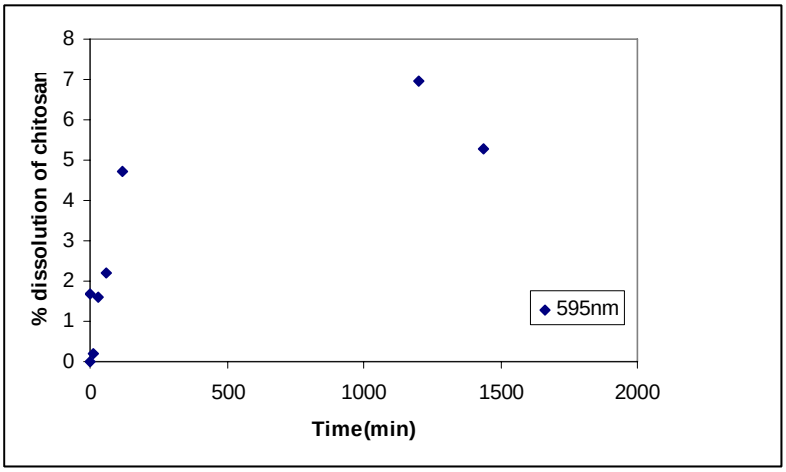

Figure 6.15. Chitosan dissolution of C50H50 at pH=5.7

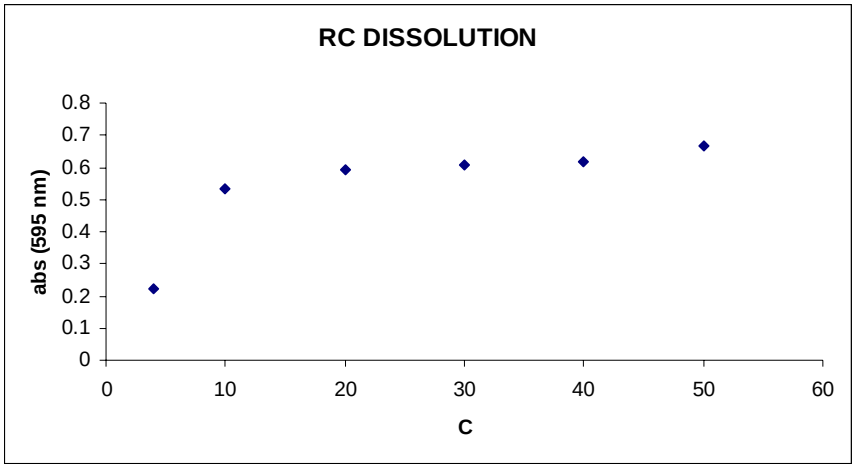

Figure 6.16. Chitosan concentration versus absorbance reading with varying amounts of raw chitosan at 595 nm (bradford method)

The BSA uptake of pure freeze-dried chitosan C100H0, C70H30, C50H50, C30H70, and pure HA powder in the pH=5.7 and pH=7.4 phosphate buffers were determined by two methods (280 nm and 595 nm Bradford) and are given in the form of bar graphs in Figures 6.17. and 6.18. It is clearly evident in both graphs that the 595 nm Bradford UV-based protein concentration determination results in sligtly higher uptake levels than the 280 nm based method which does not make use of any dyes. The freeze-dried composites have sligtly higher uptake values compared to the unprocessed as-received raw chitosan at pH=7.4. The uptake levels can reach up to about 55-60 mg/g range in the 595 nm method and to the 40-60 mg/g range for the 280 nm method. The uptake levels at pH=7.4 for the C70H30 and C50H50 composites are relatively higher than the pure freeze-dried chitosan and significantly higher than the raw as-received flaked chitosan. This is most likely due to the structural changes occurring during freeze drying and the introduction of the second phase into the composite and the significantly higher surface area generated during the preparation compared to the raw chitosan.

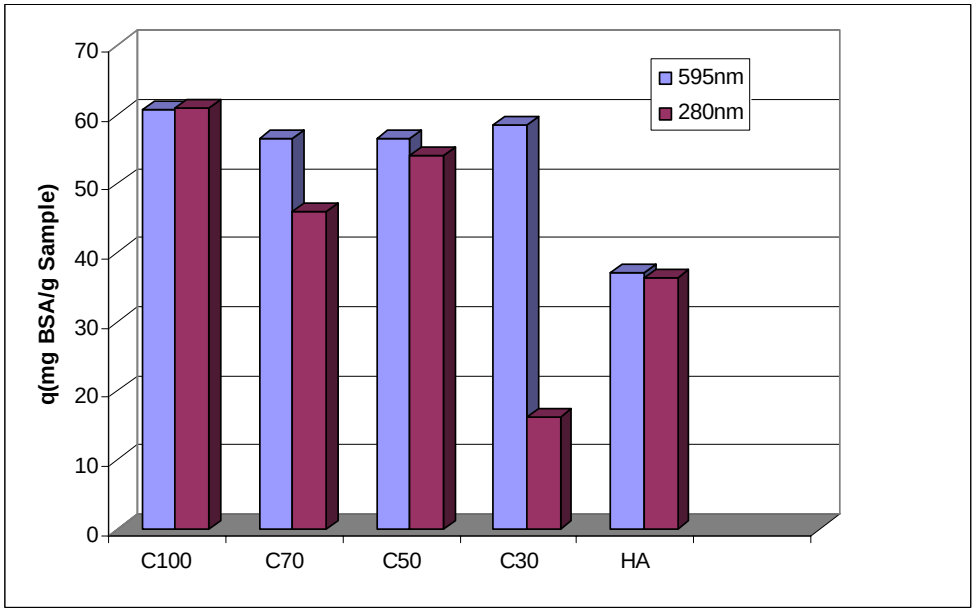

Figure 6.17. Comparison of BSA uptake at 3 hours pH=5.7 for composites and HA powder at 595nm and 280nm

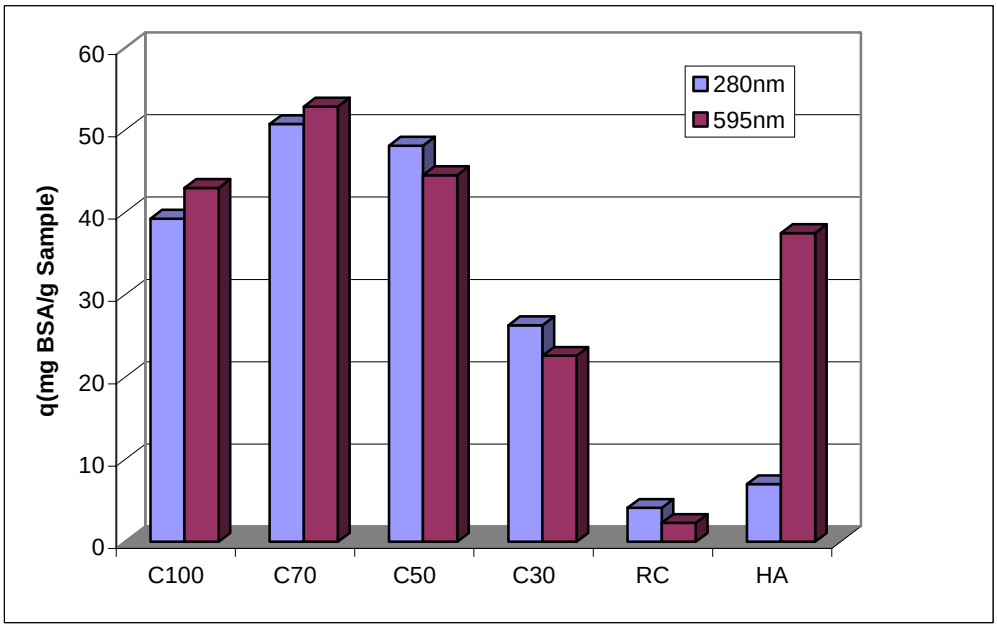

Figure 6.18. Comparison of BSA uptake at 3 hours pH=7.4 for composites and HA powder at 595nm and 280nm

The BSA uptake of composites and HA powder pretreated by soaking in about 2 ml of 0.1M NaOH and 99.5% ethanol for 1 hour in SBF (pH=7.4) is given in Figures 6.19. and 6.20. for 280 nm and 595 nm Bradford methods respectively. The uptake of BSA by these composites were significantly lower in SBF solutions than the previously discussed pH=5.7 and pH=7.4 buffer solutions. The BSA uptake values were in the 6-8 mg/g and 10-22 mg/g ranges for 280 nm and 595 nm Bradford methods respectively compared to the 40-60 mg/g and 45-60 mg/g ranges discussed previously for the pH=7.4 and pH=5.7 buffer solutions. This represents approximately 6-10 fold decreases in the BSA uptake levels in SBF solutions. The reasons for this significant difference at pH=7.4 may be likely to be due to the differences in the chemistry of the two solutions. There were also differences in the BSA uptake behaviour of the composites with the nature of pretreatment as can be seen from Figures 6.19. and 6.20. The one hour soaking in ethanol causes in general for all composites slightly higher BSA uptakes. The uptake values determined by using the 595 nm Bradford method as previously stated were significantly higher than the 280 nm method in the SBF solutions, too.

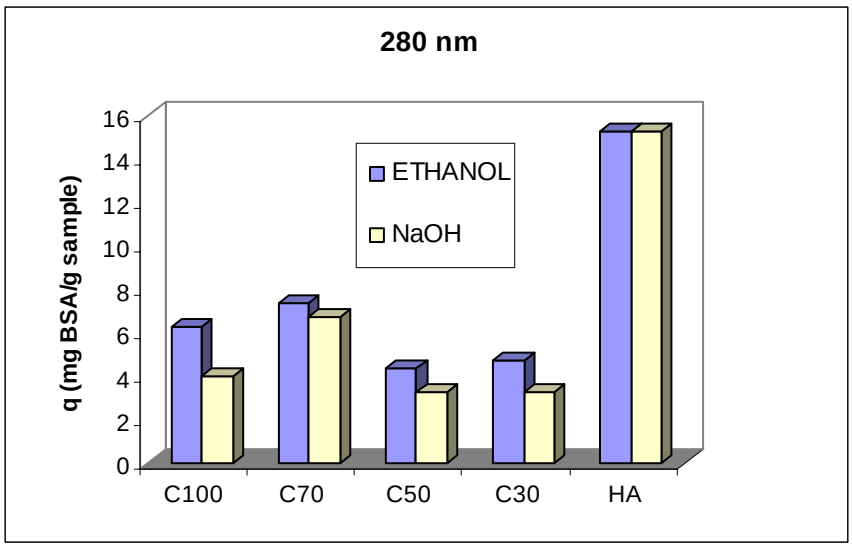

Figure 6.19. BSA uptake at 3 hours in SBF (pH=7.4) for composites and HA powder treated with NaOH and Ethanol

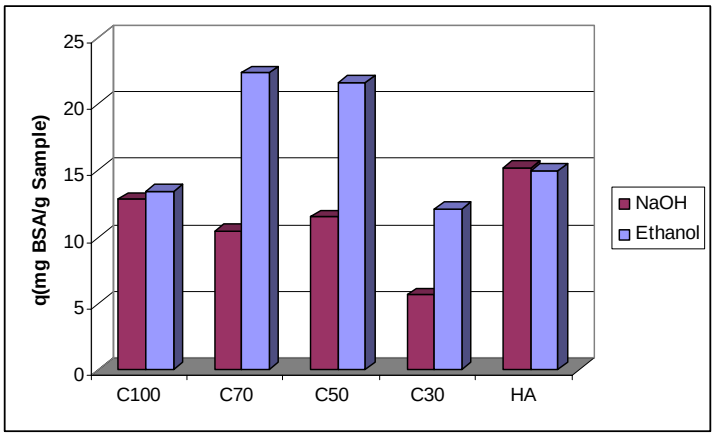

Figure 6.20. Compare of BSA uptake at 3 hours in SBF (pH=7.4) for composites and HA powder treated with Ethanol and NaOH (595 nm)

The BSA adsorption isotherms of C100H0 and C70H30 at pH= 7.4 buffer is seen in Figures 6.21. and 6.22. for 280 nm method. The BSA uptake of composites increased as the initial concentration of BSA solution increased. The adsorption isotherms of the composite materials determined in this work mostly didn't have an acceptable fit to the commonly known adsorption isotherms of Langmuir and Freundlich. The composites investigated in this work were not regular solid adsorbents (with fixed boundary/adsorption surface/adsortion site number and nature) but had a swelling nature with most likely increasing surface area/adsortion site nature and numbers during the course of BSA/HSP adsorption process. The unstability in the isotherms along with their unfavourable nature can most probably be explained with the structure of these freeze-dried biodegradable composites.

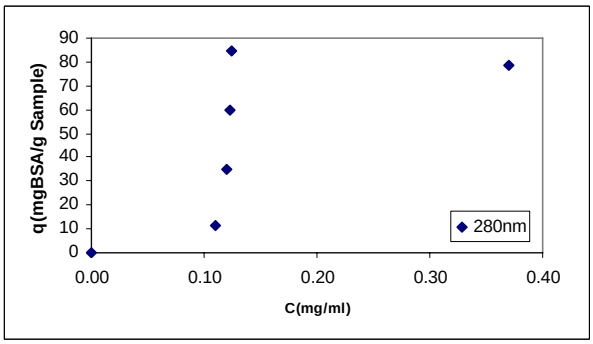

Figure 6.21. Adsorption isotherm of C100H0 at pH=7.4 at 280 nm

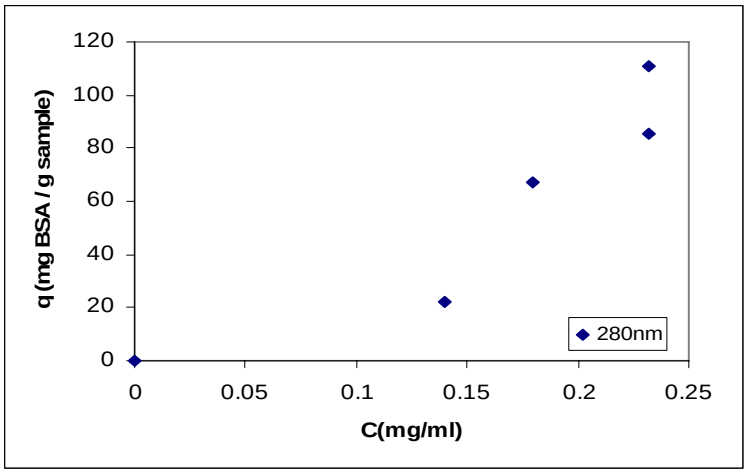

Figure 6.22. Adsorption isotherm of C70H30 at pH=7.4 at 280 nm

Adsorption isotherms of C50H50 obtained from two different sets of experiments in pH=7.4 buffer with 280 nm method is given in Figure 6.23a. The data of the first run was further fitted to a Langmuir model equation as given in Figure 23b. The 1/q vs.1/c plot for this model is further given in Figure 23c. The q_m and K values for this fit was determined as 93.46 mg/g and 0.39 mg/ml respectively.

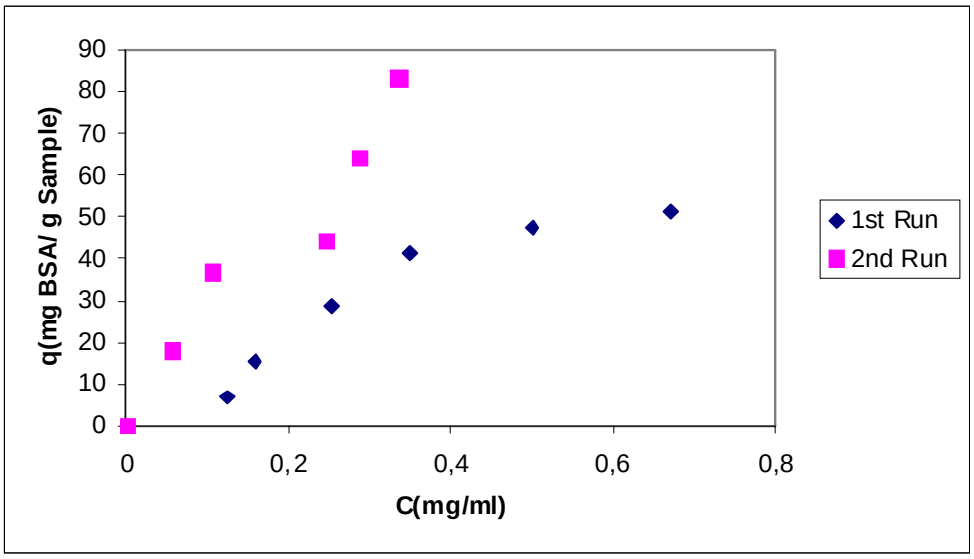

Figure 6.23a. Adsorption isotherm of C50H50 at pH=7.4 at 280 nm

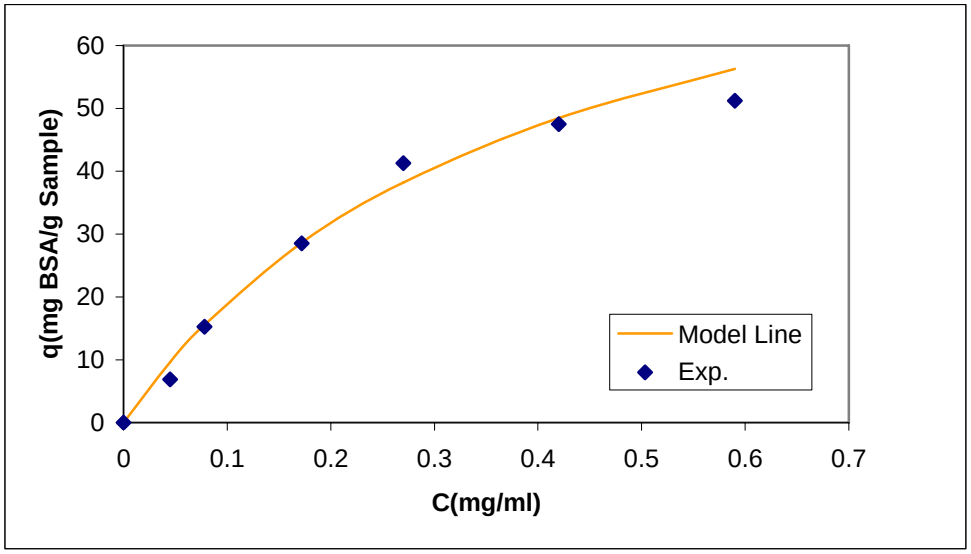

Figure 6.23b. Adsorption isotherm of C50H50 at pH=7.4 at 280 nm

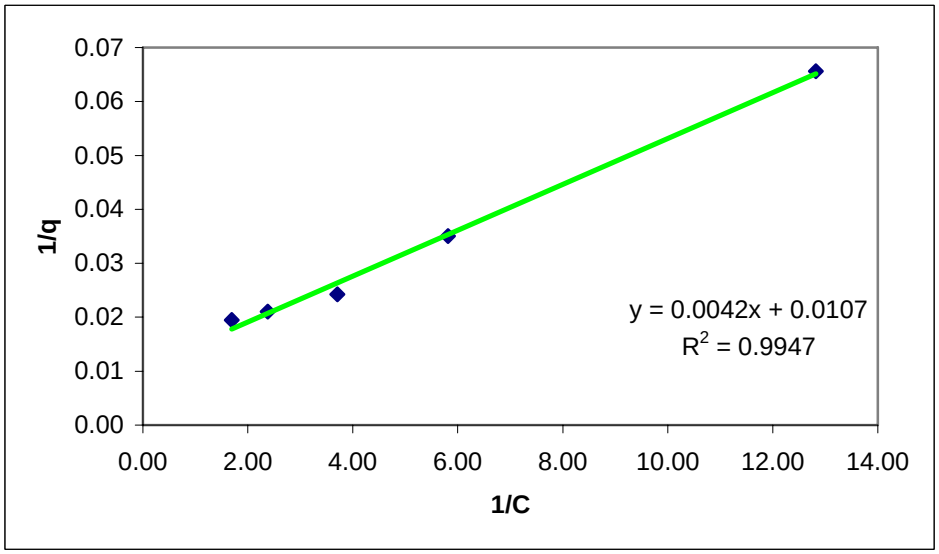

Figure 6.23c. Reciprocal plot for BSA adsorption on C50H50 at pH=7.4 at 280 nm

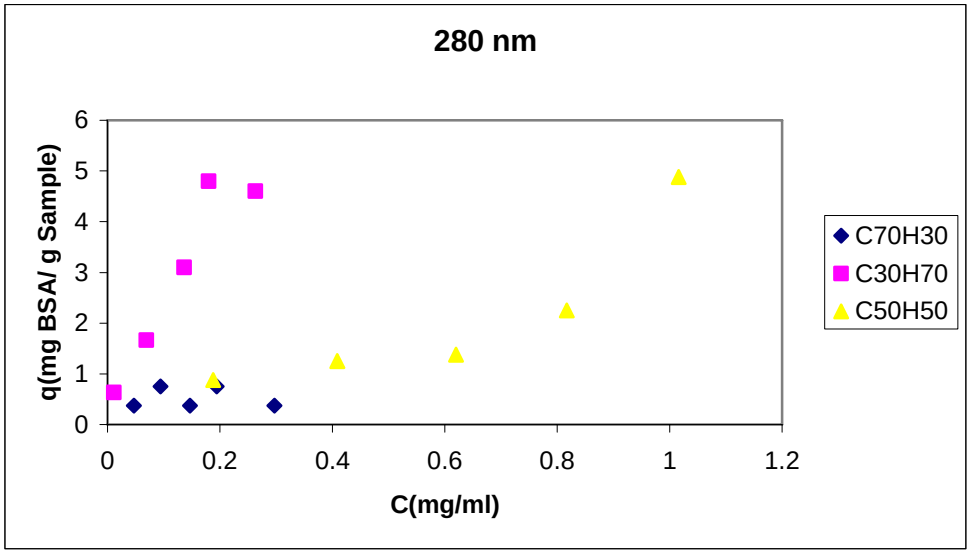

Figure 6.24. Adsorption isotherm of composites in SBF(pH=7.4) at 280 nm

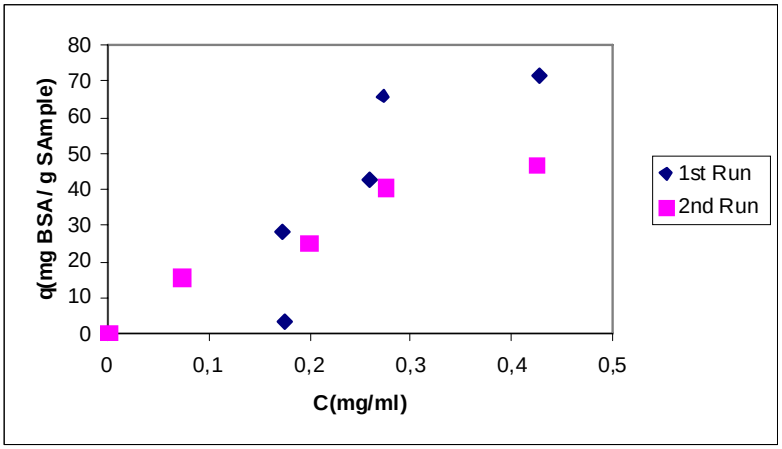

Figure 6.25. Adsorption isotherm of C50H50 at pH=7.4 at 595 nm

The uptakes of BSA by C70H30, C30H70 and C50H50 in SBF are given in Figure 6.24. The adsorption isotherms of C50H50 composite in pH=7.4 (for first and second run) are further given in Figure 6.25.

The uptake of HSP in pH=7.4 buffer by freeze-dried pure chitosan (C100H0), the three composites (C70H30, C50H50, and C30H70), raw flaked chitosan and HA at 280 nm and 595 nm is given in Figures 6.26 and 6.27. The adsorption isotherm of C50H50 composite in pH=7.4 buffer (by using the 280 nm method) is further given in

Figure 6.28. The uptake of HSP by the C50H50 and C70H30 composites is similiar with the others about 50-60 mg/g and 50-70 mg/g for 280 nm and 595 nm methods respectively. The adsorption of HSP is alot more favourable on the freeze-dried composites prepared in this work when compared with unprocessed raw flaked chitosan as is clearly seen in Figure 6.26. This may be an important advantage for these candidate scaffold biomaterials for enhanced biocompatibility.

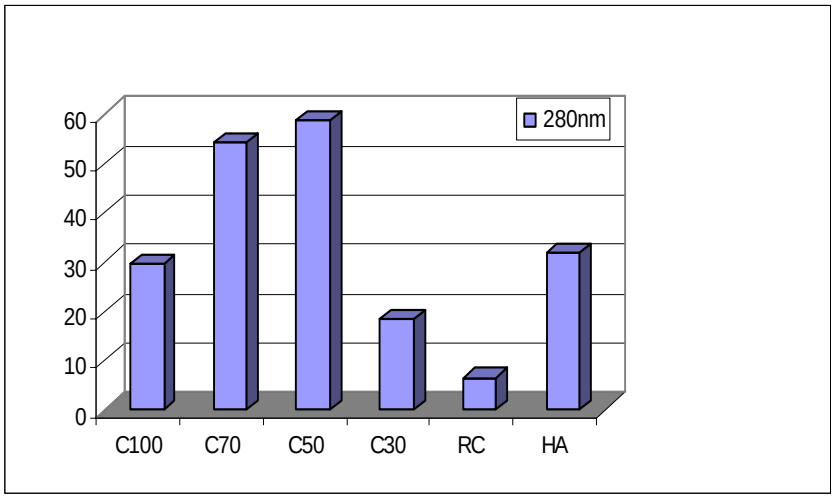

Figure 6.26. HSP uptake at 3 hours (pH=7.4) for composites

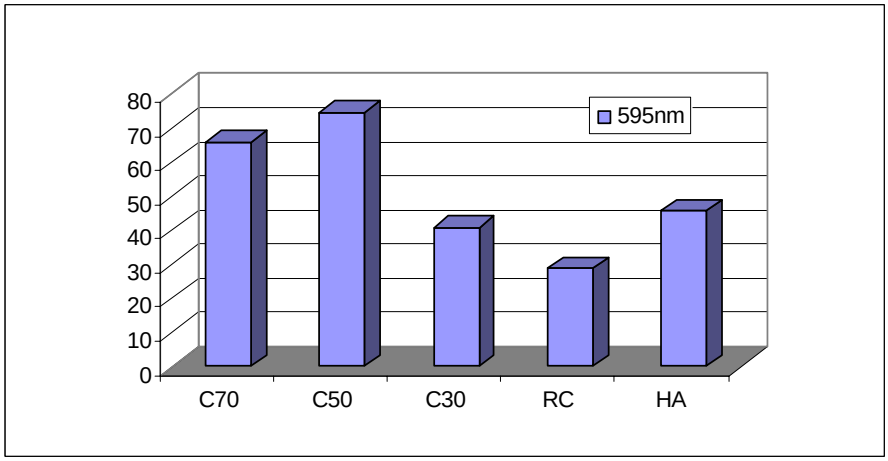

Figure 6.27. HSP uptake at 3 hours (pH=7.4) for composites

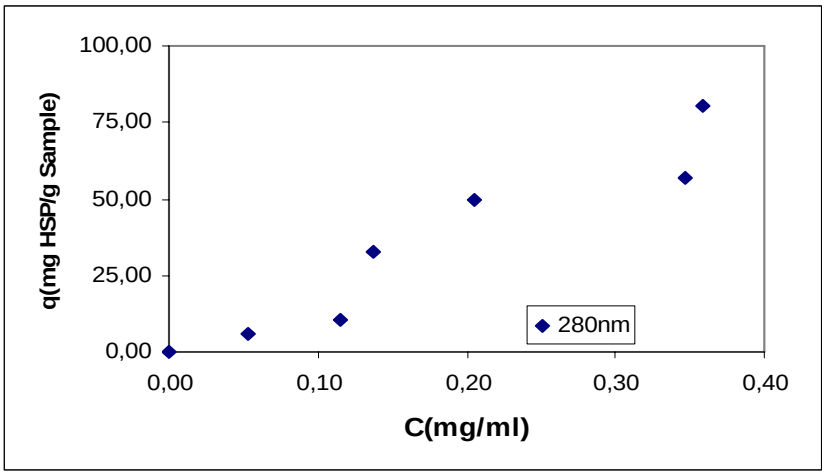

Figure 6.28. Adsorption isotherm of C50H50 at pH=7.4

CHAPTER 7

CONCLUSIONS

Biocompatibility is an essential prequisite for a successful functioning of any implant and the initial necessary phase of biocompatibility involves the adsorption of blood serum proteins onto the biomaterial surfaces which is followed by cell attachment onto the implant surfaces. Composite biomaterials formed from biodegradable chitosan biopolymer and the inorganic component of natural bone presents a unique combination for scaffold resorbable biomaterials. The preparation and characterization of porous chitosan/hydroxyapatite porous scaffold composites was conducted by freeze drying and BSA and HSP adsorption onto these scaffolds were investigated in this work.

Porous scaffolds with seven different Chitosan/HA contents with 93.5-96.3% porosity was prepared. The SEM images showed that the composites have a homogeneous and porous microstructure with pore sizes in the 50-250μ range The TGA curves have shown that the freeze dried phase separation induced biopolymer structure degrades at lower temperatures faster than the original raw polymer.

Two different UV based protein concentration determination methods, the 595 nm Bradford method which involved the use of dye solutions and the direct absorption at 280 nm by the protein solution, were used in this work. The adsortion uptake values obtained by these methods were a little different with the Bradford method and the 280 nm method determinations. Due to the use of dyes, dilutions during UV absorbance measurements, and the operator dependent nature of the 595 nm Bradford method, it is believed that the direct protein solution absorbance UV absorbance based 280 nm method was more reliable and accurate. The BSA absorption kinetics studies have shown that the equilibrium may be reached in about 2-3 hours with as high as 40-60 mg/g BSA adsorption on the scaffolds by the 280 nm method. The equilibrium adsorption behaviour of these composites didn't fit to the commonly known Langmuir and Freundlich isoterms except in one run. The swelling/degradation tendency of the biopolymer in the buffer solutions and the unstable nature of the adsorption surface/its chemical nature was held responsible for the observed adsorption behaviour. An

important finding of this work was the 6-10 fold lower BSA adsorption on these composites in SBF solutions than the pH=5.7 and 7.4 buffer solutions.

The composite structure must be stabilized by various techniques for accurate protein adsortion research. There has to be an optimum in the level of stalibizatioon since biodegradation/resorbtion of the scaffold may certainly be a significant advantage of these composites. The mechanical properties along with in situ bone growth and the the microstructural changes occurring during this process should be investigated in the future.

REFERENCES

Suchanek, W. and M. Yoshimura. 1998. Processing and properties of hydroxyapatite based biomaterials for use as hard tissue replacement implants. *Journal of Materials Research* 13:94-11.

Zhao, F., Yin, Y., Lu, W.W., Leong, J.C., W. Zhang, Zhang, J., Zhang, M., Yao, K. 2007. Preparation and histological evaluation of biomimetic three dimensional HA/chitosan-gelatin network composite scaffolds. in press *Biomaterials*.

Bosetti, M., Masse, A., Tobin, E., Cannas, M. 2001. Silver coated materials for external fixation devices: in vitro biocompatibility and genotoxicity. *Biomaterials* 23:887–892.

Grandjean- Laquerriere, A., Laquerriere, P., Laurent-Maquin , D., Guenounou, M., Philips , T.P. 2004. The effect of the physical characteristic of hydroxyapatite particles on human monocytes IL-18 production in vitro. *Biomaterials* 25:5921–5927.

Hu, S. G., Jou, C.H. and M.C. Yang. 2004. Biocompatibility and antibacterial activity of chitosan and collagen immobilized Poly (3-hydroxybutric acid-co-3-hydroxyvaleric acid). *Carbohydrate polymers* 58:173–179.

Ramakrishna, S., Mayer, J., Wintermantel, E., Leong, K.W. 2001. Biomedical applications of polymer-composite materials: a review. *Composites Science* 61:1189-1224.

Pariente, J. L., Bordeneva, L., Vallı, N., Bareille, R. 1998. An in vitro biocompatibility evaluation of double –J stents. *Urolog* 52:524-530.

Zhang, Y. and M. Zhang. 2001. Synthesis and characterization of macroporous chitosan/calcium phosphate composite scaffolds for tissue engineering. *Journal of Biomedical Material Research* 55:304-312.

Park, J. and Lakes, R.S., eds. 1992. *Biomaterials: An introduction*. Plenum Press.

Zhao, F., Song, X.F., Yao, K.D., Lu, W.W., Leong, C. 2007. Preparation and Characterization of Hydroxyapatite/Chitosan-Gelatin Network Composite. *Journal of Applied Polymer Science* 77:2929–2938.

Wang, X., Ma, J., Wang, Y., He, B. 2001. Structural characterization of phosphorylated chitosan and their applications as effective additives of calcium phosphate cements. *Biomaterial* 22: 2247-2255.

Hench, L.L. and Wilson J., eds. 1993. *An Introduction to Bioceramics*. World Scientific.

Zhang, Y. and M. Zhang. 2001. Microstructural and mechanical characterization of chitosan scaffolds reinforced by calcium phosphates. *Journal of Non-Crystalline Solids* 282:159-164.

Varma, H.K., Yokogawa, Y., Espinosa F.F., Kawamoto, Y., Nishizawa, K., Nagata, F., Kameyama, T. 1999. Porous calcium phosphate coating over phosphorylated chitosan film by a biomimetic method. *Biomaterials* 20:879-884.

Kandori, K., Tsuyamaa, S., Tanaka, H., Ishikawa, T. 2007. Protein adsorption characteristics of calcium hydroxyapatites modified with pyrophosphoric acids. *Colloids and Surfaces B: Biointerfaces* 58:98–104.

Rouahi, M., Championb, E., Gallet, O., Jada , A., Anselme, K. 2006. Physico-chemical characteristics and protein adsorption potential of hydroxyapatite particles: Influence on in vitro biocompatibility of ceramics after sintering. *Colloids and Surfaces B: Biointerfaces* 47:10–19.

Latour, Robert A. Jr. 2005. *Biomaterials: Protein–Surface Interactions*. South Carolina, U.S.A. Bioengineering Books.

Zhoua, X., Sunb, Y., Liu, Z. 2007. Superporous pellicular agarose–glass composite particle for protein adsorption. *Biochemical Engineering Journal* 34:99–106.

Lousinian, S. and S. Logothetidis. 2007. Optical properties of proteins and protein adsorption study. *Biomaterials: Protein–Surface Interactions* 84:479–485.

Hench L.L. 1998. Bioceramics. *J.Am. Ceramic Soc*. 81:1705–1728.

Manjubala, I., Scheler, S. and K.D. Jandt, 2006. Mineralisation of chitosan scaffolds with nano-apatite formation by double diffusion technique. *Acta Biomaterialia* 2:75–84

Aguilar, M.D.A., Espinosa, S., Rodriguez, L., Pina, C. 1999. Biocompatibility in vitro tests of Zinalco. *Mutation Research* 446:129–133.

Risbud, M. and D.N. Saheb. 2001. Preparation, characterization and in vitro biocompatibility evaluation of poly (butylene terphthalate)/ wollastonite composites. *Biomaterials* 22:1591–1599.

Hoven, V.P., Tangpasuthadol, V., Angkitpaiboon, Y., Vallapa, N., Kiatkamjornwong S. 2007. Surface-charged chitosan: Preparation and protein adsorption. *Carbohydrate Polymers* 68: 44–53.

Wang, Y., Wang, X., Luo, G., Dai, Y. 2007. Adsorption of bovin serum albumin (BSA) onto the magnetic chitosan nanoparticles prepared by a microemulsion system. *Bioresource Technology*.

Zhao, F., Grayson, W.L., Ma, T., Bunnell, B., Lu, W.W. 2006. Effects of hydroxyapatite in 3-D chitosan–gelatin polymer network on human mesenchymal stem cell construct development. *Biomaterials* 27:1859–1867.

APPENDIX A

STANDARD CURVES FOR PROTEIN ABSORPTION

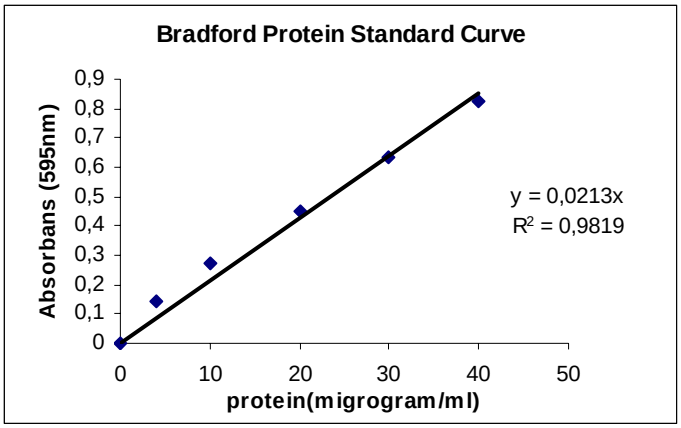

Figure A.1. BSA 595 nm Bradford method standard calibration curve

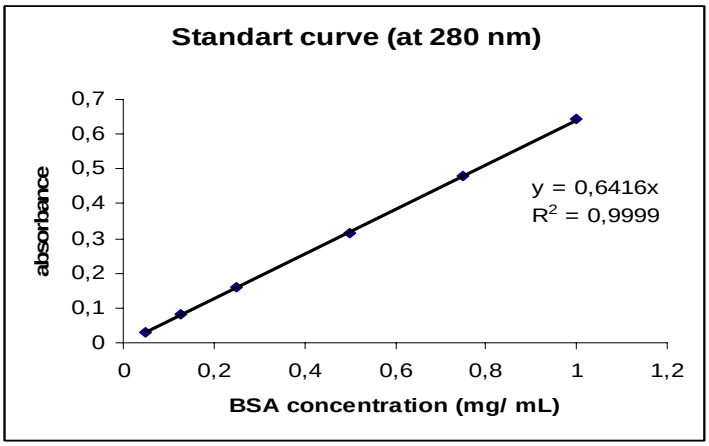

Figure A.2. BSA 280 nm standard calibration curve

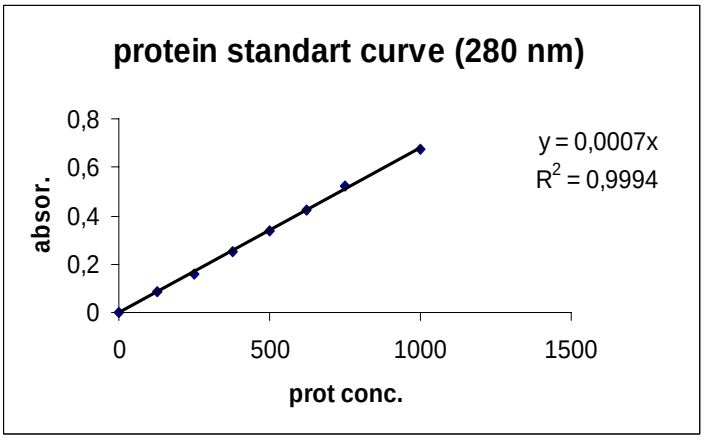

Figure A.3. HSP 280 nm standard curve